Electronic Supplementary Material (ESI) for Chemical Communications.

Supporting Information

Stereoelectronically-Induced Allosteric Binding: Shape Complementarity Promotes Positive Cooperativity in Fullerene / Buckybowl Complexes

Eric S. Larsen,[a,b] Guillermo Ahumada,[a] Prakash R. Sultane[a]

and Christopher W. Bielawski[*a,b]*

[a] Center for Multidimensional Carbon Materials (CMCM), Institute for Basic Science (IBS), Ulsan 44919, Republic of Korea

[b] Department of Chemistry, Ulsan National Institute of Science and Technology (UNIST), Ulsan 44919, Republic of Korea

Table of Contents

General Considerations

Unless otherwise specified, all reagents were purchased from commercial sources and used without further purification. Copper iodide, hydrogen chloride solution (4.0 M in 1,4-dioxane), *N*,*N*-diisopropylethylamine, 2,3-dichloro-5,6-dicyano-1,4-benzoquinone, 1,8-diazabicyclo[5.4.0]undec-7-ene, and *N*,*N*-dimethylacetamide were purchased from Sigma-Aldrich. 1-chloro-2-iodobenzene was purchased from Alfa Aesar. Potassium carbonate, anhydrous magnesium sulfate, sodium chloride, and anhydrous sodium sulfate were purchased from Daejung Chemicals. Tetrakis(triphenylphosphine)palladium ($Pd(PPh_3)_4$), palladium (II) acetate, and di-*t*-butyl(methyl)phosphonium tetrafluoroborate were purchased from Strem. 2,6-dichlorobenzaldehyde was purchased from TCI. 2,6-dibromoaniline was purchased from Activate Scientific. 2-(hydroxymethyl)phenylboronic acid cyclic monoester was purchased from AK Scientific, Inc. Deuterated benzene, toluene, chloroform, and dimethyl sulfoxide were purchased from Cambridge Isotope Laboratories, Inc. C_{60} (99.99%) was purchased from BuckyUSA. The solvents that were used inside of the glovebox were dried and degassed using a Vacuum Atmospheres solvent purification system. 1,8-diazabicyclo[5.4.0]undec-7-ene and *N*,*N*-dimethylacetamide were independently sparged with nitrogen and dried over molecular sieves (< 20 ppm H_20 as determined by Karl Fischer titration) and then transferred into the glovebox. Dimethyl(1-diazo-2-oxopropyl)phosphate (the Bestmann-Ohira reagent) was prepared according to a literature procedure.[1]

^1H and ^{13}C NMR data were recorded using a Bruker 400 MHz spectrometer. Titration and Diffusion data were recorded using either a Bruker 400 MHz spectrometer or a Varian 600 MHz spectrometer. Chemical shifts (δ) are reported in ppm and are referenced to the residual solvent (^1H: C_6D_6, 7.16 ppm; $CDCl_3$, 7.26 ppm; DMSO-d_6, 2.50 ppm; toluene-d_8, 7.09 ppm; ^{13}C: C_6D_6, 128.06 ppm; $CDCl_3$, 77.16 ppm; DMSO-d_6, 39.52 ppm; toluene-d_8, 137.86 ppm).[2] Coupling constants (*J*) are expressed in hertz (Hz). Splitting patterns are denoted as follows: br, broad; s, singlet; d, doublet; t, triplet; q, quartet; m, multiplet. High resolution mass spectra (HRMS) were recorded with a Waters Xevo G2-XS Q-ToF

using the electrospray ionization (ESI) or atmospheric pressure chemical ionization (APCI) mode. Infrared (FT-IR) spectra were recorded on an Agilent Cary 630 spectrometer equipped with an attenuated total reflectance (ATR) attachment (diamond). UV-vis spectra were acquired using an Agilent Cary 100 UV-vis Spectrometer. 6Q Spectrosil® quartz cuvettes (Starna) with 1.0 cm path lengths were used. Melting points were obtained using a Stanford Research Systems MPA100 OptiMelt automated melting point apparatus and are uncorrected. Reactions requiring microwave irradiation were performed in an Anton-Paar Microwave Synthesis Reactor Monowave 300.

Synthetic Procedures

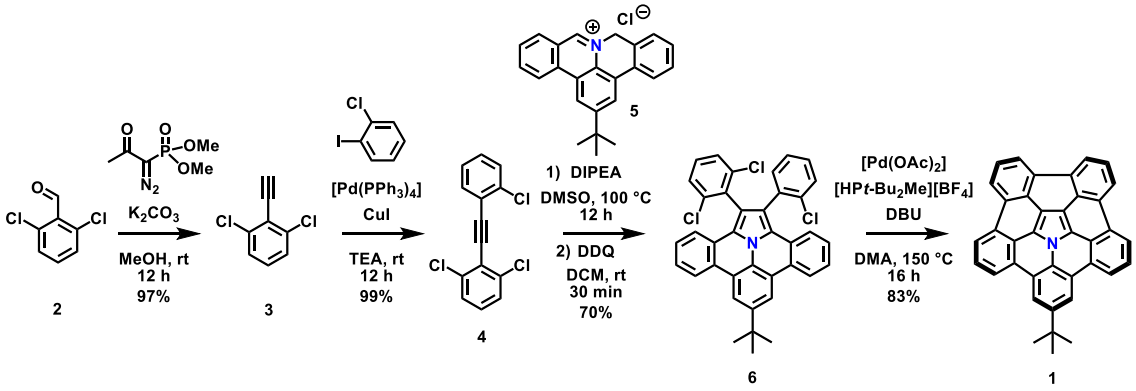

Scheme S1. The synthetic route that was used to prepare azacorannulene **1**.

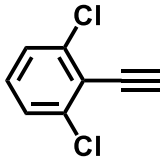

1,3-Dichloro-2-ethynylbenzene (3). Following a literature procedure,[3] a 1 L round bottom flask was charged with 2,6-dichlorobenzaldehyde (10.01 g, 57.0 mmol), freshly prepared dimethyl(1-diazo-2-oxopropyl)phosphonate (15.23 g, 80.0 mmol, 1.4 equiv.), potassium carbonate (31.71 g, 228.0 mmol, 4.0 equiv.) and methanol (540 mL). The flask was then sealed with a rubber septum that was first attached to an oil bubbler via a needle and the solution was vigorously stirred at room temperature for 12 h. Note: The reaction produces nitrogen and needs to be properly ventilated to avoid a potentially dangerous build-up of pressure. Afterward, water was added (270 mL) and the layers were separated and extracted with pentane (3 × 485 mL). The collected organic layers were dried over anhydrous magnesium sulfate and filtered, and the residual solvent was removed under reduced pressure to afford a white, crystalline solid (9.46 g, 97% yield). Spectral data agreed with literature values.[4] **m.p** 96-98 °C (lit. 97-99 °C); **^{1}H NMR** (400 MHz, $CDCl_3$): δ 7.34 (d, *J* = 8.3 Hz, 2H), 7.20 (t, *J* = 8.7Hz, 1H), 3.68 (s, 1H); **^{13}C NMR** (100 MHz, $CDCl_3$): δ 138.0, 129.7, 127.7, 122.4, 88.0, 77.4; **^{1}H NMR** (400 MHz, DMSO-d_6): δ 7.57 (d, *J* = 8.2 Hz,

2H), 7.43 (t, *J* = 8.7Hz, 1H), 4.97 (s, 1H); **^{13}C NMR** (100 MHz, DMSO-d_6): δ 136.6, 130.9, 128.1, 121.2, 91.8, 77.0; **IR** (ATR): 3286 (C≡C–H), 3075, 1428, 1191, 776, 717, 666 cm^{-1}.

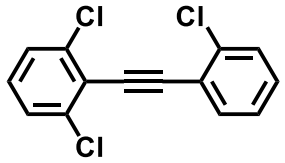

1,3-Dichloro-2-((2-chlorophenyl)ethynyl)benzene (4). Following a literature procedure,[5] a 100 mL round bottom flask was charged with 1,3-dichloro-2-ethynylbenzene (**3**) (2.09 g, 11.7 mmol), 1-chloro-2-iodobenzene (3.32 g, 14.0 mmol, 1.2 equiv.), $Pd(PPh_3)_4$ (0.71 g, 0.6 mmol, 0.051 equiv.), triethylamine (22 mL) and a stir bar inside of a glovebox. Under vigorous stirring, CuI (0.22 g, 1.2 mmol, 0.1 equiv.) was added in one shot to the flask and then stirred at room temperature for 12 h. The reaction was then removed from the glove box, filtered and the precipitate was washed with triethylamine (3 × 40 mL). The residual solvent was removed under reduced pressure and the crude material was allowed to stand overnight. The crude solid was dissolved in minimal dichloromethane and run through a silica plug eluting with a 2:8 (*v*/*v*) mixture of dichloromethane:hexane. The residual solvent was removed under reduced pressure to afford a white, crystalline solid (3.4 g, 99 % yield). Spectral data agreed with literature values.[6] **m.p.** 78-80 °C (lit. 73.6-74.6 °C); **^{1}H NMR** (400 MHz, $CDCl_3$): δ 7.65 (dd, *J* = 7.5, 1.9 Hz, 1H), 7.46 (dd, *J* = 7.9, 1.4 Hz, 1H), 7.37 (d, *J* = 8.0 Hz, 2H), 7.34 – 7.25 (m, 2H), 7.20 (dd, *J* = 8.6, 7.7 Hz, 1H); **^{13}C NMR** (100 MHz, $CDCl_3$): δ 137.6, 136.3, 133.9, 130.1, 129.6, 129.5, 127.7, 126.6, 123.2, 122.8, 96.5, 88.4; **^{1}H NMR** (400 MHz, DMSO-d_6): δ 7.72 (dd, *J* = 7.6, 1.7 Hz, 1H), 7.67 – 7.60 (m, 3H), 7.55 – 7.41 (m, 3H); **^{13}C NMR** (100 MHz, DMSO-d_6): δ 136.2, 134.8, 133.7, 131.2, 131.1, 129.6, 128.2, 127.5, 121.5, 121.2, 95.9, 87.8; **IR** (ATR): 1550, 1482, 1421, 1191, 1048, 757 cm^{-1}.

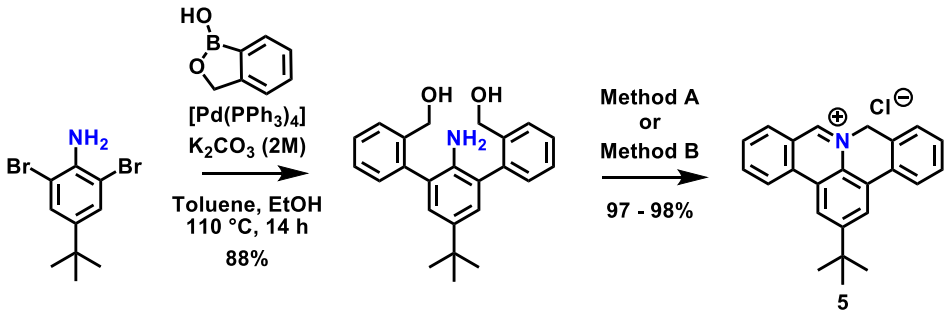

Scheme S2. Synthetic route used to synthesize iminium chloride salt **5**.

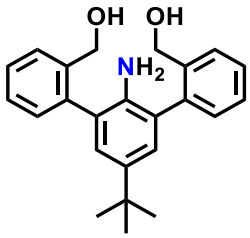

4-*t*-Butyl-2,6-bis[(2'-hydroxymethyl)phenyl]aniline. A 1000 mL, 3-neck round bottom flask was charged with 2,6-dibromoaniline (5.45 g, 17.8 mmol), 2-(hydroxymethyl)phenylboronic acid cyclic monoester (7.32 g, 53.4 mmol, 3.0 equiv.), $Pd(PPh_3)_4$ (2.951 g, 2.5 mmol, 0.14 equiv.) and a stir bar inside of a glovebox. The flask was then fitted with a Dimroth condenser, sealed with rubber septa and removed from the glovebox. In a separate 1000 mL round bottom flask equipped with a stir bar was added 436.5 mL toluene, 87 mL ethanol, and 169 mL of a 2.0 M K_2CO_3 aqueous solution. The resulting mixture was then sparged with nitrogen for 30 min while vigorously stirring. This solution was then transferred via cannula to the 3-neck flask and refluxed for 14 h. The reaction was cooled to room temperature and the organic layer was separated and the aqueous layer was extracted with diethyl ether (3 × 250 mL). The combined organic layers were washed with saturated sodium chloride, dried over magnesium sulfate and excess solvent removed under reduced pressure. The resulting crude material was purified by column chromatography eluting with a 1:2 (*v*/*v*) mixture of hexane:ethyl acetate to afford a brown colored resin after residual solvent was removed under reduced pressure (5.64 g, 88% yield). Spectral data agreed with literature values.[7, 8] **m.p**. 140-143 °C (lit. 143-147°C); **^{1}H NMR** (400 MHz, $CDCl_3$): δ 7.59 – 7.53 (m, 2H), 7.46 – 7.37 (m, 4H),

7.36 – 7.27 (m, 2H), 7.13 (d, *J* = 5.1 Hz, 2H), 4.49 – 4.38 (m, 4H), 1.30 (d, *J* = 2.7 Hz, 9H); **^{13}C NMR** (100 MHz, $CDCl_3$): δ 144.5, 139.8, 139.5, 137.9, 137.8, 130.8, 130.3, 129.9, 129.8, 129.3, 129.1, 128.9, 128.8, 128.6, 127.00, 126.9, 63.9, 63.7, 34.5, 34.4, 31.7; **^{1}H NMR** (400 MHz, DMSO-d_6): δ 7.62 (d, *J* = 7.6 Hz, 2H), 7.40 (t, *J* = 7.5 Hz, 2H), 7.33 (t, *J* = 7.4 Hz, 2H), 7.22 – 7.15 (m, 2H), 6.92 (d, *J* = 2.5 Hz, 2H), 5.08 (t, *J* = 5.5 Hz, 1H), 5.04 (t, *J* = 5.3 Hz, 1H), 4.45 – 4.24 (m, 4H), 3.50 (d, *J* = 14.9 Hz, 2H), 1.25 (s, 9H); **^{13}C NMR** (100 MHz, DMSO-d_6): δ 140.9, 140.7, 139.0, 138.9, 138.9, 138.7, 137.3, 137.1, 129.8, 129.6, 127.4, 127.4, 127.1, 126.9, 126.7, 125.9, 125.8, 125.1, 60.6, 60.3, 33.6, 31.5; **IR** (ATR): 3321, 3060, 2953, 2866, 1611, 1459, 1362, 1242, 1036, 1003, 886, 769, 735cm^{-1}; **HRMS (ESI)**: *m/z* calcd for $C_{24}H_{27}NO_2Na$ $[M+Na]^+$ 384.1939, found 384.1961.

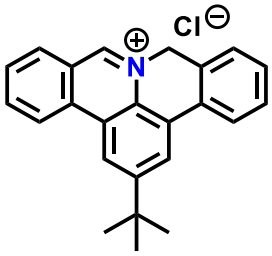

2-*t*-Butyl-8-hydroisoquinolino[4,3,2-*de*]phenanthridin-9-ium chloride (5). *Method A:* To a 30 mL Anton Parr microwave tube equipped with a stir bar was added 4-*t*-butyl-2,6-bis[(2'-hydroxymethyl)phenyl]aniline (515 mg, 1.35 mmol), 4.63 mL of a hydrogen chloride solution (4.0 M HCl in 1,4-dioxane, 13.7 equiv.) and sealed with Anton Parr septum cap. The vessel was placed in the microwave and run at 130 °C for 90 min (MW details: heat as fast as possible to 130 °C, stirred at 750 (rpm), vessel removed at 30 °C). Afterward, the cap was removed inside of a fume hood, placed on a stir plate, and allowed to stir overnight under a stream of air. The concentrated solution was diluted with diethyl ether which produced a yellow precipitate. The mixture was sonicated until a uniform dispersion was observed, then filtered and washed with diethyl ether (3 × 10 mL). The product was dried under reduced pressure to afford a bright yellow solid (494 mg, 98% yield). *Method B:* To a 100 mL pressure tube equipped with a stir bar was added 4-*t*-butyl-2,6-bis[(2'-hydroxymethyl)phenyl]aniline (508 mg, 1.35 mmol), 4.63 mL of a hydrogen chloride solution (4.0 M HCl in 1,4-dioxane, 13.7 equiv.). The tube was then sealed and

placed in a 130 °C oil bath for 20 h. The reaction vessel was removed from the oil bath and allowed to stir overnight under a stream of air. The concentrated solution was diluted with diethyl ether which produced a yellow precipitate. The mixture was sonicated until a uniform dispersion was observed, and then filtered and washed with diethyl ether (3 × 10 mL). The product was dried under reduced pressure to afford a bright yellow solid (479 mg, 97% yield). Spectral data for the compounds obtained using either method agreed with literature values.[7, 9] **m.p.** 138-142 °C (lit. 140 °C); **^{1}H NMR** (400 MHz, $CDCl_3$): δ 11.96 (s, 1H), 8.99 (d, *J* = 8.1 Hz, 1H), 8.75 (d, *J* = 8.4 Hz, 1H), 8.65 (d, *J* = 1.6 Hz, 1H), 8.51 (d, *J* = 1.6 Hz, 1H), 8.26 (t, *J* = 7.7 Hz, 1H), 8.00 (m, 2H), 7.65 (d, *J* = 7.0 Hz, 1H), 7.59 – 7.49 (m, 2H), 6.58 (s, 2H), 1.59 (s, 9H); **^{13}C NMR** (100 MHz, $CDCl_3$): δ 154.6, 154.4, 137.9, 134.5, 130.6, 130.5, 129.7, 128.3, 127.9, 127.4, 127.3, 127.2, 126.5, 124.9, 123.6, 123.4, 122.4, 119.2, 57.4, 36.1, 31.4; **^{1}H NMR** (400 MHz, DMSO-d_6): δ 10.22 (s, 1H), 9.29 (d, *J* = 8.4 Hz, 1H), 8.93 (d, *J* = 1.6 Hz, 1H), 8.76 (d, *J* = 1.6 Hz, 1H), 8.63 (d, *J* = 7.7 Hz, 1H), 8.49 – 8.44 (m, 1H), 8.41 (t, *J* = 7.7 Hz, 1H), 8.13 (t, *J* = 7.6 Hz, 1H), 7.64 – 7.56 (m, 3H), 6.23 (s, 2H), 1.58 (s, 9H); **^{13}C NMR** (100 MHz, DMSO-d_6): δ 154.00, 153.3, 137.7, 134.0, 132.4, 130.5, 129.8, 129.2, 128.3, 128.2, 127.1, 126.4, 126.2, 126.00, 124.3, 124.1, 123.8, 123.5, 119.9, 56.9, 35.9, 30.9; **IR** (ATR): 3058, 2955, 2868, 1626, 1603, 1530, 1501, 1421, 1354, 1242, 1054, 876, 786, 754 cm^{-1}; **HRMS (ESI)**: *m/z* calcd for $C_{24}H_{22}N$ $[M\text{-}Cl]^+$ 324.1747, found 324.1778.

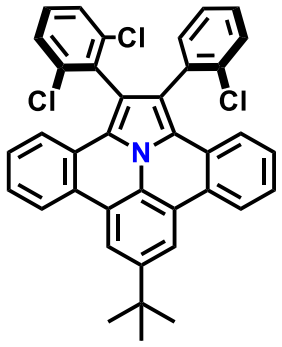

8-*t*-Butyl-1-(2-chlorophenyl)-2-(2,6-dichlorophenyl)benzo[7,8]indolizino[6,5,4,3-*def*]phenanthridine (6). In a glovebox, a 250 mL round bottom flask was charged with **5** (2.46 g, 7.1 mmol), **4** (4.27 g, 14.2 mmol, 2.1 equiv.) and 100 mL of dimethyl sulfoxide ($[\mathbf{5}]_0$ = 0.07 M). Separately, a syringe was charged with N,N-diisopropylethylamine (2.9 mL,

16.5 mmol, 2.33 equiv.) and capped with a clean septum. The flask and syringe were removed from the glovebox and the flask was placed in an oil bath that was thermostatted to 100 °C. When the solids had fully dissolved, the contents of the syringe were added to the flask in one shot and the reaction was allowed to stir for 12 h. The reaction was cooled to room temperature, diluted with toluene, and transferred to a separatory funnel. Water (500 mL) was then added and extracted with toluene until the organic layer was no longer UV active. The combined organic layers were dried with anhydrous sodium sulfate and the residual solvent was removed under reduced pressure. The crude contents were transferred to a 300 mL round bottom flask and inserted into a glove box. The flask was then charged with 142 mL of dichloromethane (0.05 M with respect to the iminium salt) and 2,3-dichloro-5,6-dicyano-1,4-benzoquinone (1.61 g, 7.1 mmol, 1.0 equiv.), and then stirred for 30 min. The flask was removed from the glovebox, washed with a saturated aqueous solution of sodium bicarbonate, and extracted with dichloromethane. After removal of residual solvent, the crude product was purified by silica gel column chromatography, wherein pentane was used first to recover **4** followed by a 1:8 (*v*/*v*) mixture of dichloromethane:hexane to afford **6** as a bright yellow solid (2.9 g, 70% yield). Spectral data agreed with literature values.[10] **m.p.** >300 °C (lit. 273-275 °C); **^{1}H NMR** (400 MHz, $CDCl_3$): δ 8.47 – 8.37 (m, 4H), 7.51 – 7.36 (m, 6H), 7.33 (dd, *J* = 8.1, 1.2 Hz, 1H), 7.30 – 7.16 (m, 6H), 1.58 (s, 9H); **^{13}C NMR** (100 MHz, $CDCl_3$): δ 146.6, 137.8, 137.5, 136.00, 134.7, 134.6, 132.7, 129.8, 129.6, 128.9, 128.6, 128.4, 128.3, 128.2, 127.9, 126.9, 126.7, 126.6, 126.4, 126.3, 123.5, 122.9, 122.7, 122.7, 122.6, 122.5, 117.7, 116.5, 35.5, 32.0; **^{1}H NMR** (400 MHz, DMSO-d_6): δ 8.71 (t, *J* = 7.7 Hz, 2H), 8.60 (s, 2H), 7.66 (dd, *J* = 8.0, 1.2 Hz, 1H), 7.59 (dd, *J* = 7.9, 1.1 Hz, 1H), 7.55 – 7.28 (m, 10H), 7.10 (d, *J* = 8.1 Hz, 1H), 1.57 (s, 9H); **^{13}C NMR** (100 MHz, DMSO-d_6): δ 147.3, 136.7, 136.0, 134.7, 133.6, 133.2, 131.9, 131.00, 129.8, 129.0, 128.6, 128.6, 128.3, 127.1, 127.00, 126.9, 125.7, 125.5, 125.5, 125.4, 123.9, 123.7, 122.3, 121.7, 121.6, 121.5, 121.0, 120.1, 118.3, 117.9, 116.0, 35.3, 31.5; **IR** (ATR): 3063, 3040, 2956, 2904, 1610, 1573, 1557, 1438, 1251, 1192, 1064, 1039, 869, 784, 746,729 cm^{-1}; **HRMS (ESI)**: *m/z* calcd for $C_{38}H_{26}Cl_3N$ $[M]^+$ 601.1131, found 601.1166.

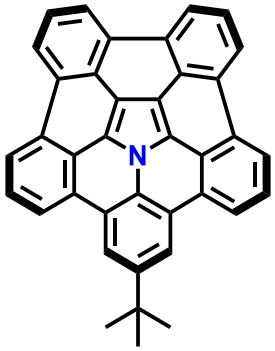

8-*t*-Butyl-6b^2-azadibenzo[*fg*,*ij*]benzo[5,6]acenaphtho[4,3,2,1,8,7-*pqrstuv*]pentaphene or 8-*t*-butyl-6b^2-azapentabenzo[*bc*,*ef*,*hi*,*kl*,*no*]corannulene (1). In a glovebox, a 50 mL round bottom flask was charged with **6** (255 mg, 0.4 mmol), palladium acetate (108 mg, 0.4 mmol, 1.0 equiv.), di-t-butyl(methyl)phosphonium tetrafluoroborate (321 mg, 1.2 mmol, 3.01 equiv.), 1,8-diazabicyclo[5.4.0]undec-7-ene (4.6 mL, 30.3 mmol, 73.0 equiv.), 11 mL of N,N-dimethylacetamide ([**6**]$_0$ = 0.0368 M) and a stir bar. The flask was sealed with a rubber septum and copper-wired shut. The flask was then removed from the glove box and sparged with N_2 for 10 min under vigorous stirring. The flask was then sealed and placed in an oil bath thermostatted to 150 °C and stirred for 16 h. The solution was cooled to room temperature and placed in a separatory funnel where 110 mL water was added. This mixture was extracted with CH_2Cl_2 once (20 mL) and the collected organic layer was set aside. Subsequent CH_2Cl_2 washes were conducted until there were no longer any UV-active compounds in the organic collections. After standing for 5-30 min, aggregation of a yellow-orange colored material appeared in the first collected organic fraction. This solution was filtered, and the material was washed with hexane and methanol (1st batch of material). The remaining collected organic layers were combined, dried over anhydrous sodium sulfate, and filtered. The flask was then attached to a rotary-evaporator and enough residual solvent was removed until a yellow-orange precipitate was observed. At this point, the flask was sonicated. The mixture was then filtered and washed with hexane and methanol (2nd batch of material). The two batches were separately dissolved in toluene and run through a silica plug, dried, and then precipitated from dichloromethane into hexane. The products collected from each bath were dried separately under reduced pressure which resulted in a bright yellow-orange solid (combined weight and yield: 172

mg, 83% yield). Spectral data agreed with literature values.[10] **m.p.** >300 °C (lit. 280-282 °C); **^{1}H NMR** (400 MHz, C_6D_6): δ 8.35 (d, *J* = 8.0 Hz, 4H), 8.31 (d, *J* = 7.7 Hz, 2H), 8.19 (s, 2H), 7.96 (d, *J* = 7.7 Hz, 2H), 7.61 (t, *J* = 7.9 Hz, 2H), 7.50 (t, *J* = 7.9 Hz, 2H), 1.46 (s, 9H); **^{13}C NMR** (100 MHz, C_6D_6): δ 133.4, 132.2, 131.1, 130.8, 129.2, 128.6, 126.1, 125.6, 125.5, 124.8, 124.3, 123.5, 123.3, 120.4, 120.00, 35.5, 32.1; **^{1}H NMR** (400 MHz, toluene-d_8): δ 8.30 (d, *J* = 8.0 Hz, 4H), 8.26 (d, *J* = 7.7 Hz, 2H), 8.16 (s, 2H), 7.93 (d, *J* = 7.7 Hz, 2H), 7.57 (t, *J* = 7.9 Hz, 2H), 7.47 (t, *J* = 7.9 Hz, 2H), 1.48 (s, 9H); **^{13}C NMR** (100 MHz, toluene-d_8): δ 133.7, 132.4, 131.3, 131.1, 126.3, 124.6, 123.8, 123.6, 120.7, 120.2, 35.9, 32.57; **^{1}H NMR** (400 MHz, CS_2 with DMSO-d_6 co-axial insert): δ 8.18 (d, *J* = 8.1 Hz, 2H), 8.12 (d, *J* = 8.0 Hz, 2H), 8.06 (d, *J* = 7.7 Hz, 2H), 7.94 (s, 2H), 7.82 (d, *J* = 7.7 Hz, 2H), 7.43 – 7.35 (m, 4H), 1.33 (s, 9H); **^{13}C NMR** (100 MHz, CS_2 with DMSO-d_6 co-axial insert): δ 191.8, 145.8, 138.3, 132.1, 131.9, 130.7, 129.6, 129.1, 127.7, 125.00, 124.7, 124.1, 124.00, 123.4, 122.5, 122.3, 119.7, 119.4, 34.6, 31.5; **IR** (ATR): 3057, 2955, 2905, 2871, 1891, 1650, 1624, 1560, 1540, 1508, 1492, 1361, 1130, 774, 745, 733 cm^{-1}; **HRMS (ESI)**: *m/z* calcd for $C_{38}H_{23}N$ $[M]^+$ 493.1830, found 493.1810. Anal. calcd. For $C_{38}H_{23}N$: C, 92.47; H, 4.70; N, 2.84; Found C, 92.25; H, 4.53; N, 2.76.

NMR Spectra

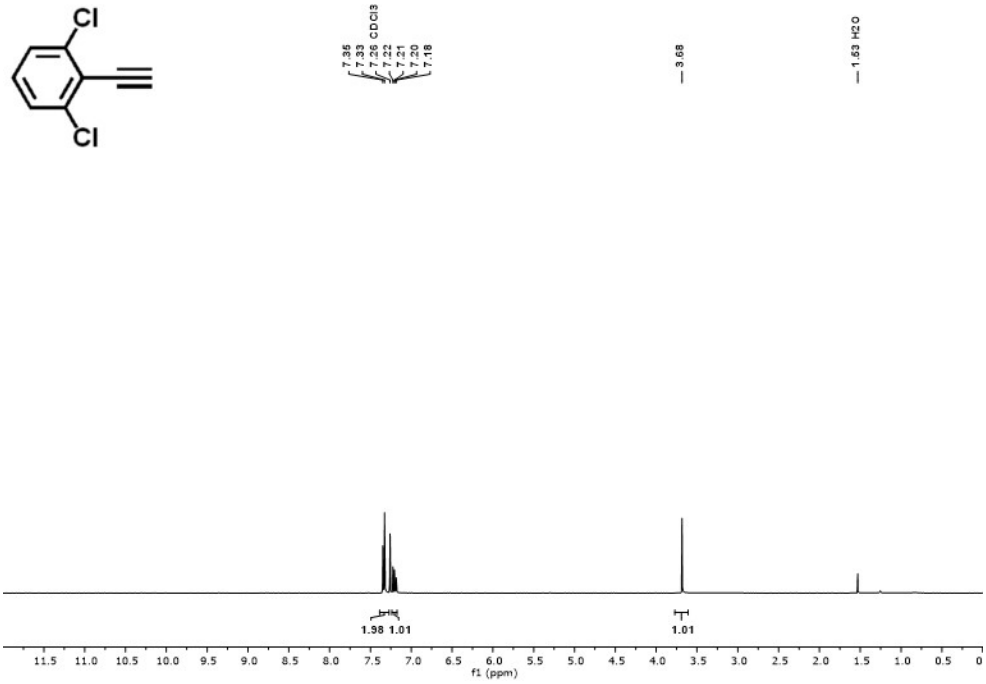

Figure S1. ^{1}H NMR spectrum recorded for **3** ($CDCl_3$).

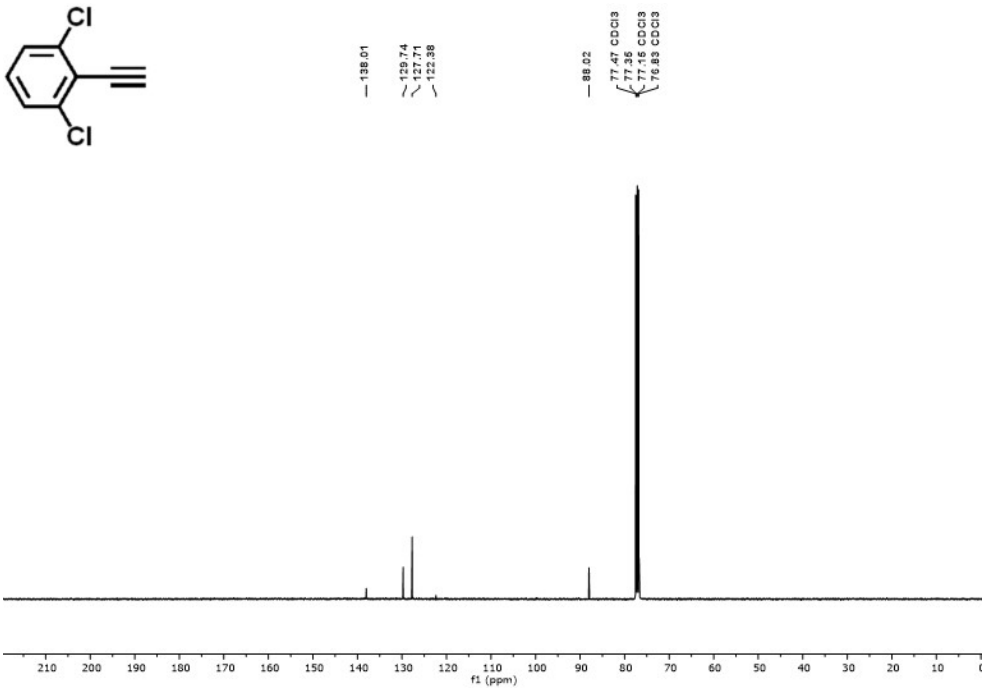

Figure S2. ^{13}C NMR spectrum recorded for **3** ($CDCl_3$).

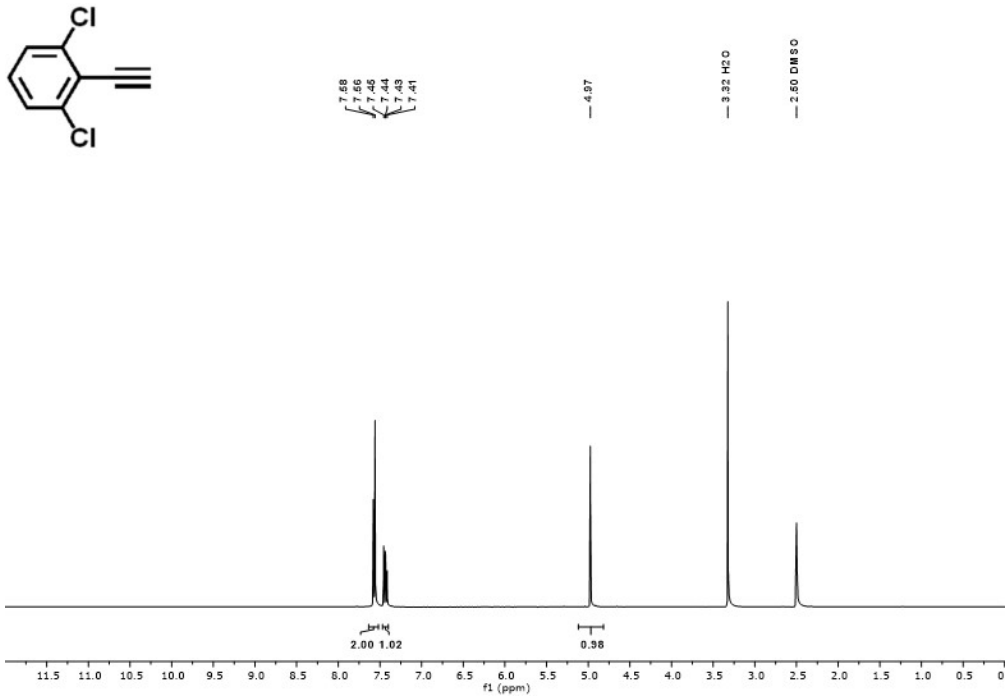

Figure S3. ^{1}H NMR spectrum recorded for **3** (DMSO-d_6).

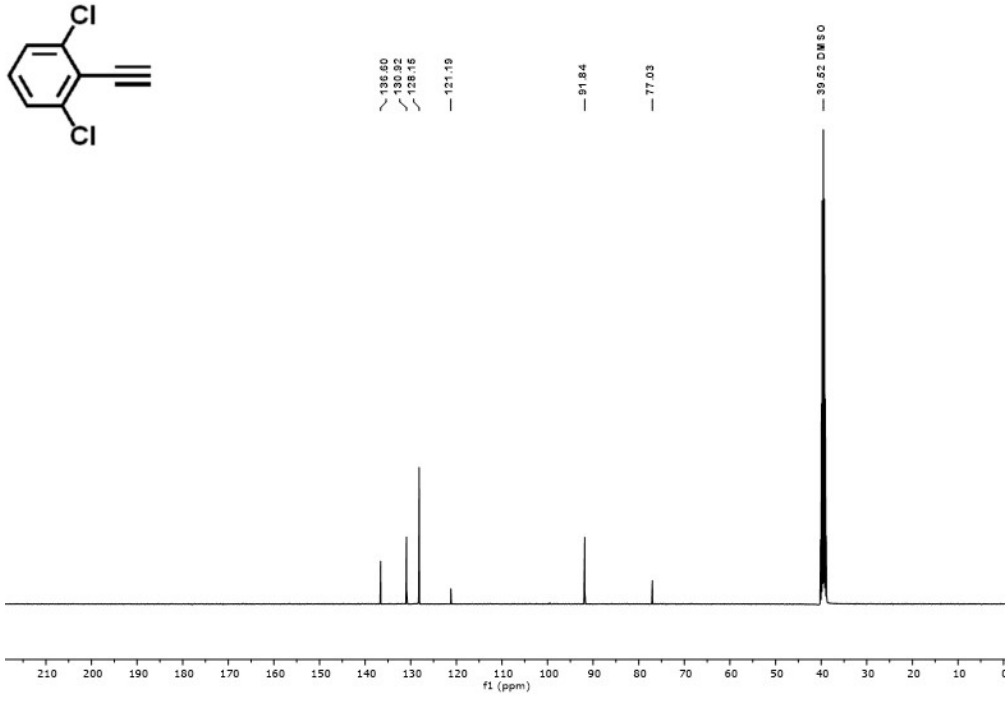

Figure S4. ^{13}C NMR spectrum recorded for **3** (DMSO-d_6).

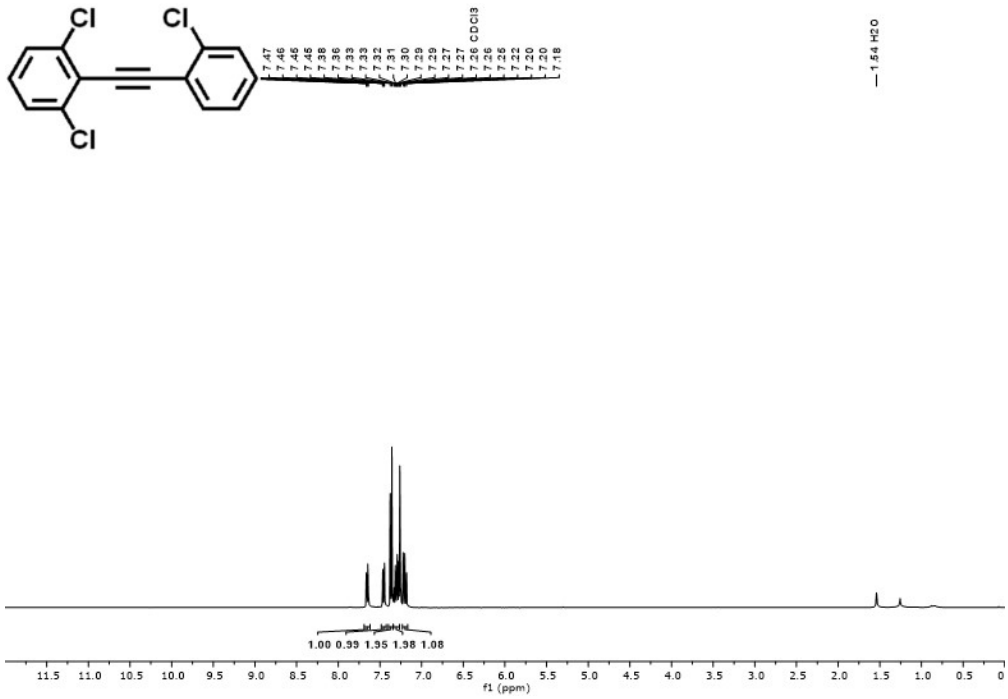

Figure S5. ^{1}H NMR spectrum recorded for **4** ($CDCl_3$).

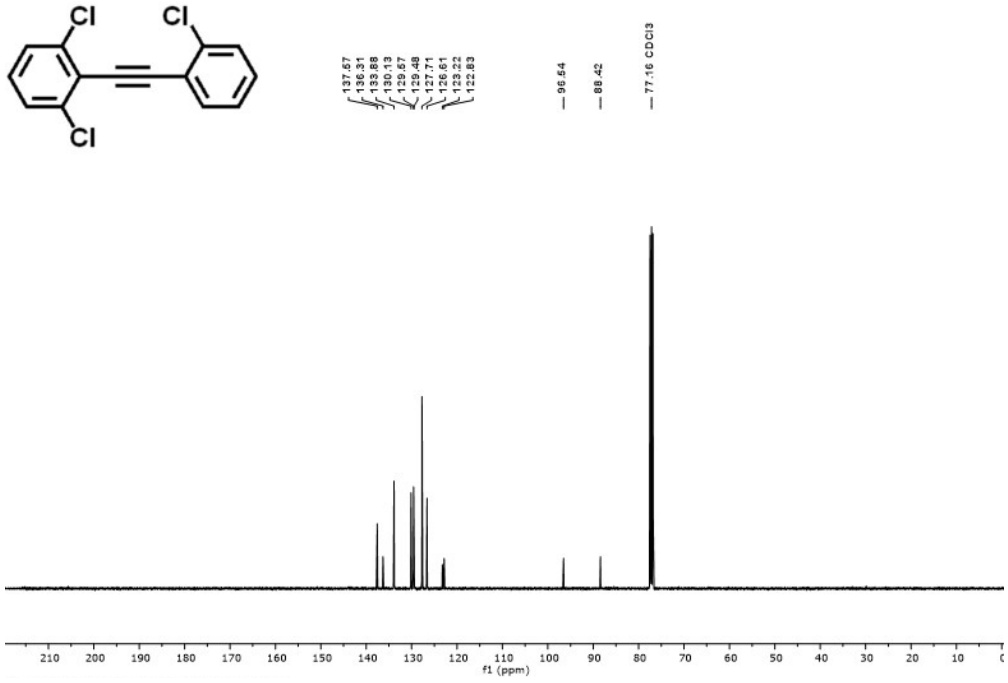

Figure S6. ^{13}C NMR spectrum recorded for **4** ($CDCl_3$).

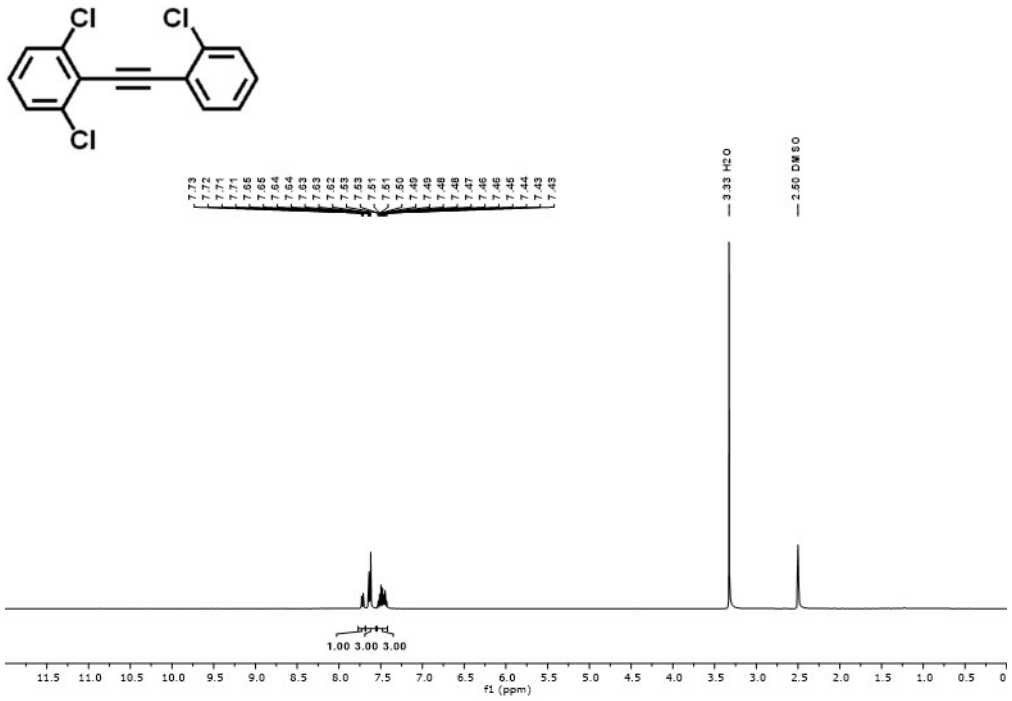

Figure S7. ^{1}H NMR spectrum recorded for **4** (DMSO-d_6).

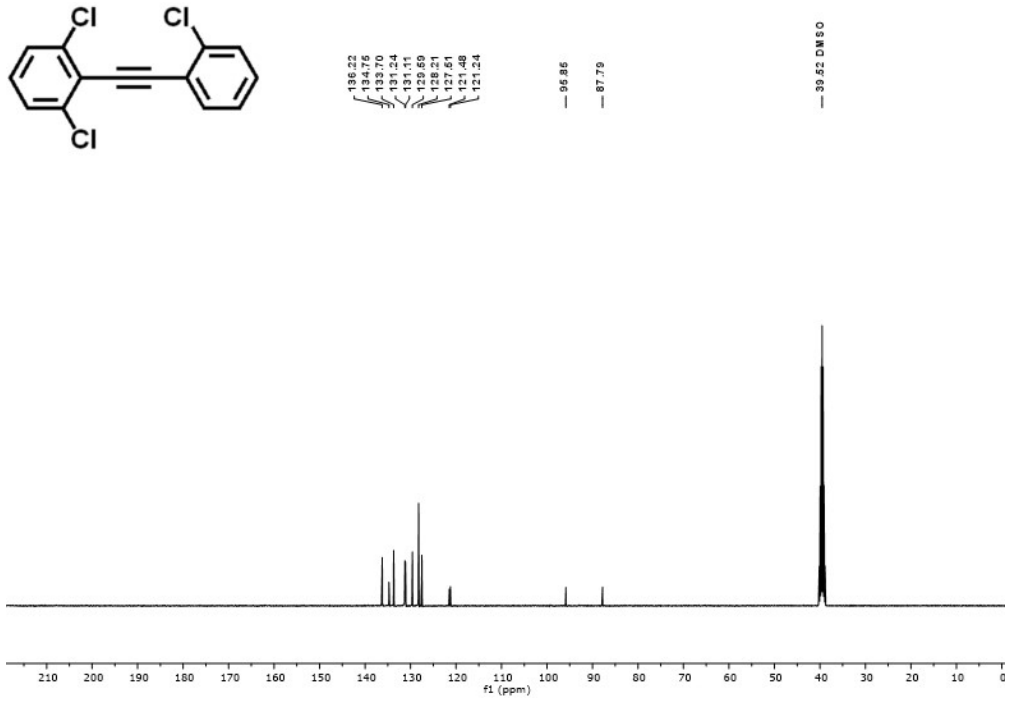

Figure S8. ^{13}C NMR spectrum recorded for **4** (DMSO-d_6).

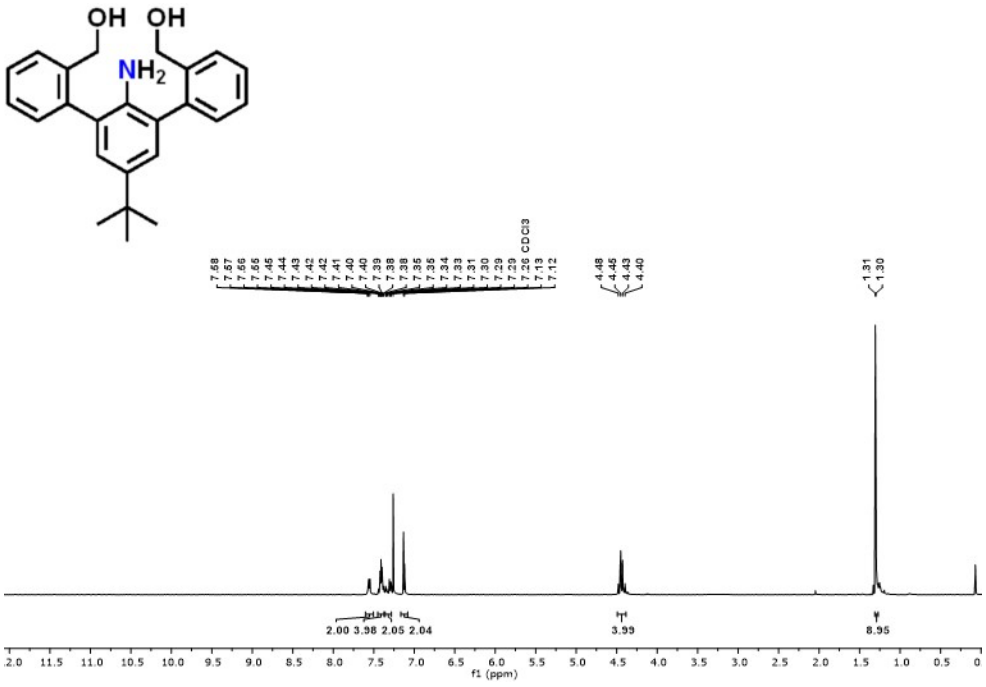

Figure S9. ^{1}H NMR spectrum recorded for 4-*t*-butyl-2,6-bis[(2'-hydroxymethyl)phenyl]aniline ($CDCl_3$).

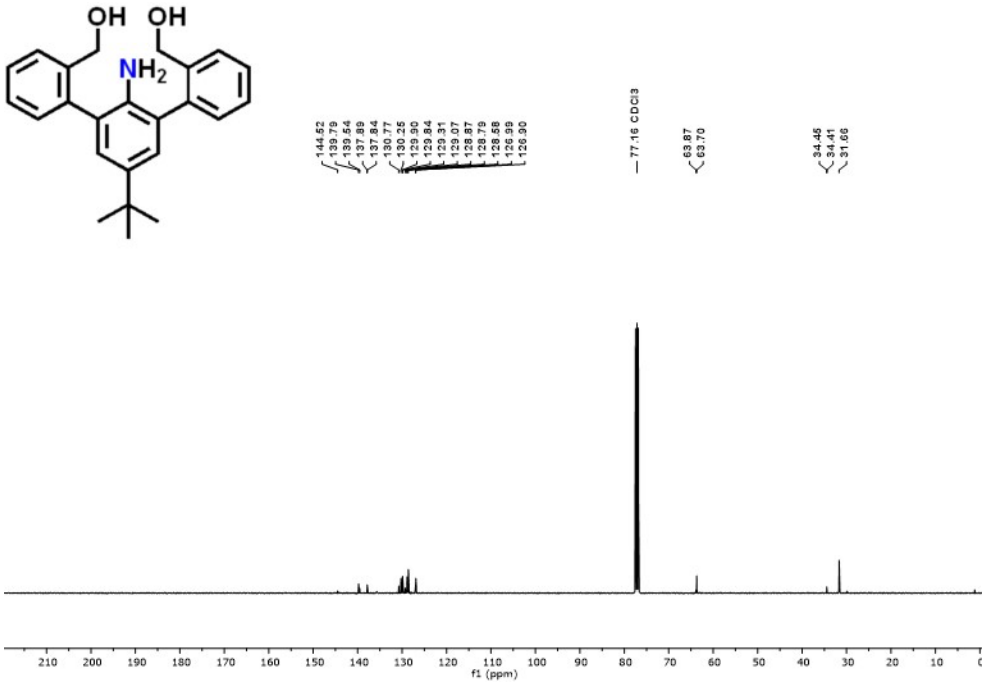

Figure S10. ^{13}C NMR spectrum recorded for 4-*t*-butyl-2,6-bis[(2'-hydroxymethyl)phenyl]aniline ($CDCl_3$).

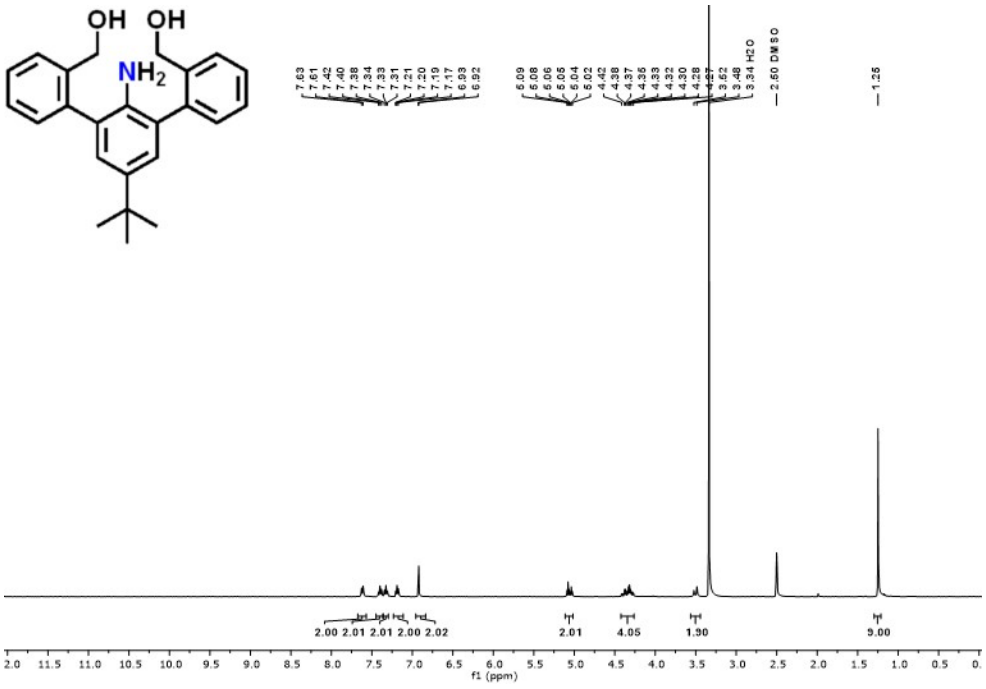

Figure S11. ^{1}H NMR spectrum recorded for 4-*t*-butyl-2,6-bis[(2'-hydroxymethyl)phenyl]aniline (DMSO-d_6).

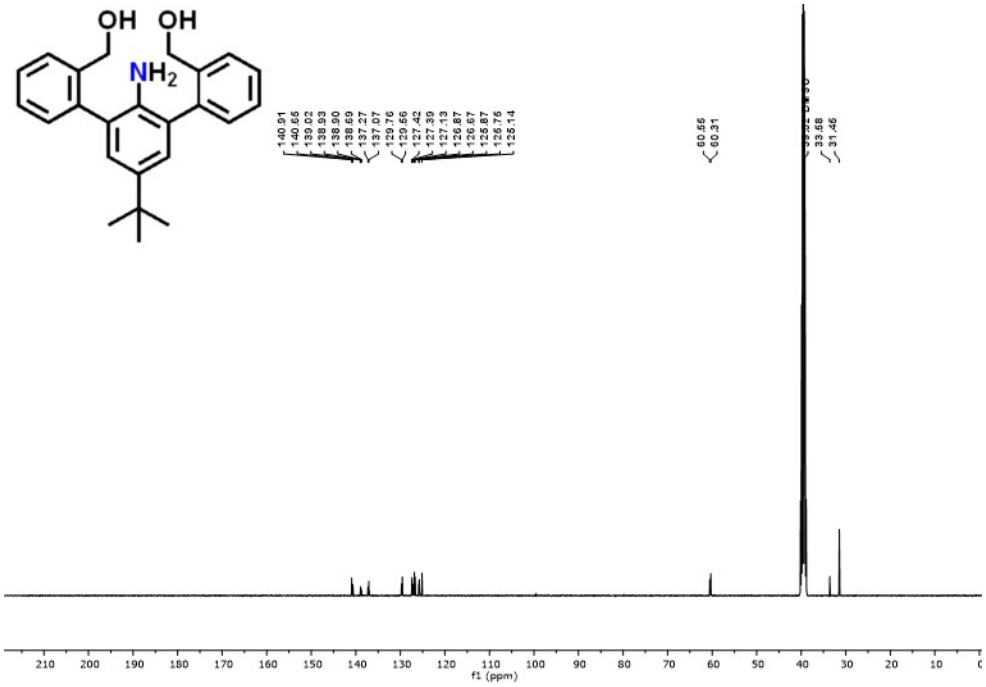

Figure S12. ^{13}C NMR spectrum recorded for 4-*t*-butyl-2,6-bis[(2'-hydroxymethyl)phenyl]aniline (DMSO-d_6).

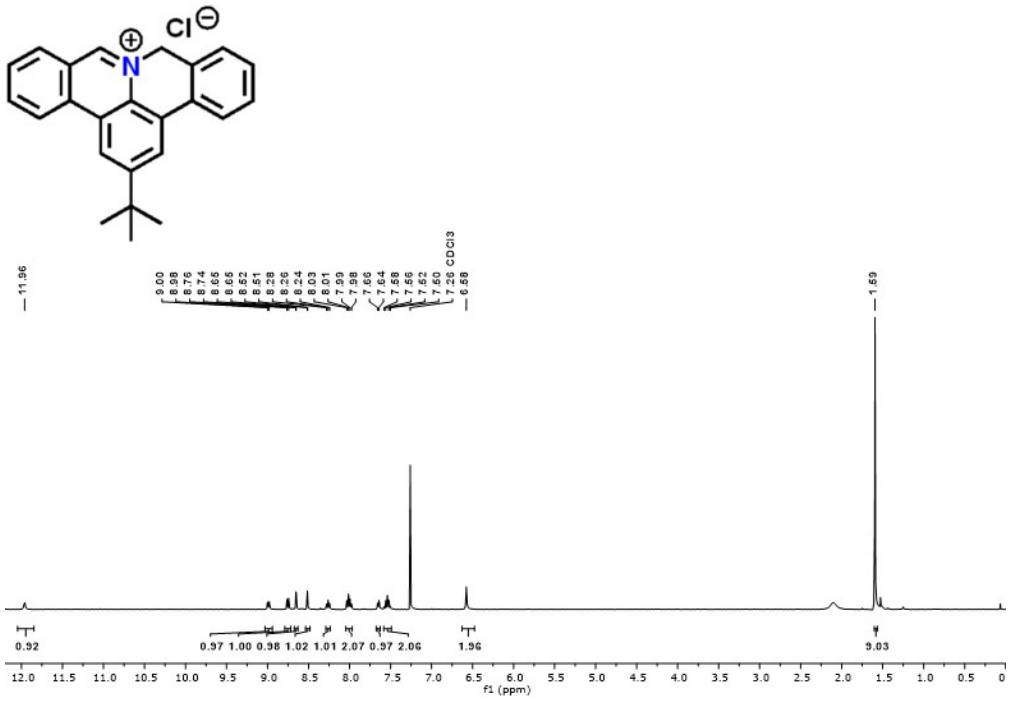

Figure S13. ^{1}H NMR spectrum recorded for **5** ($CDCl_3$).

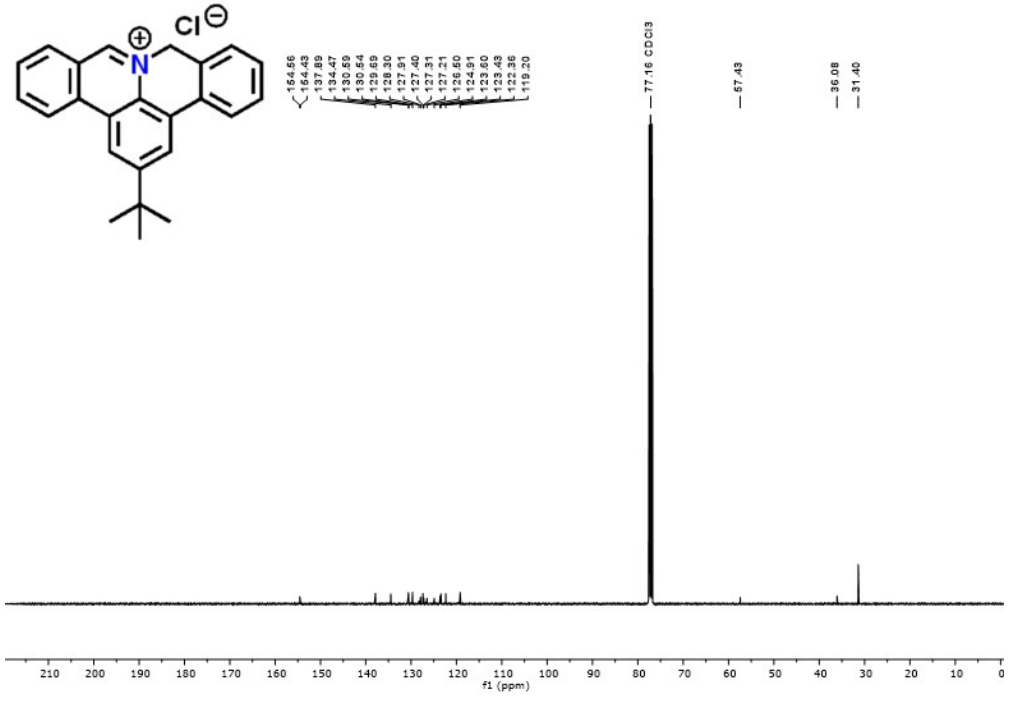

Figure S14. ^{13}C NMR spectrum recorded for **5** ($CDCl_3$).

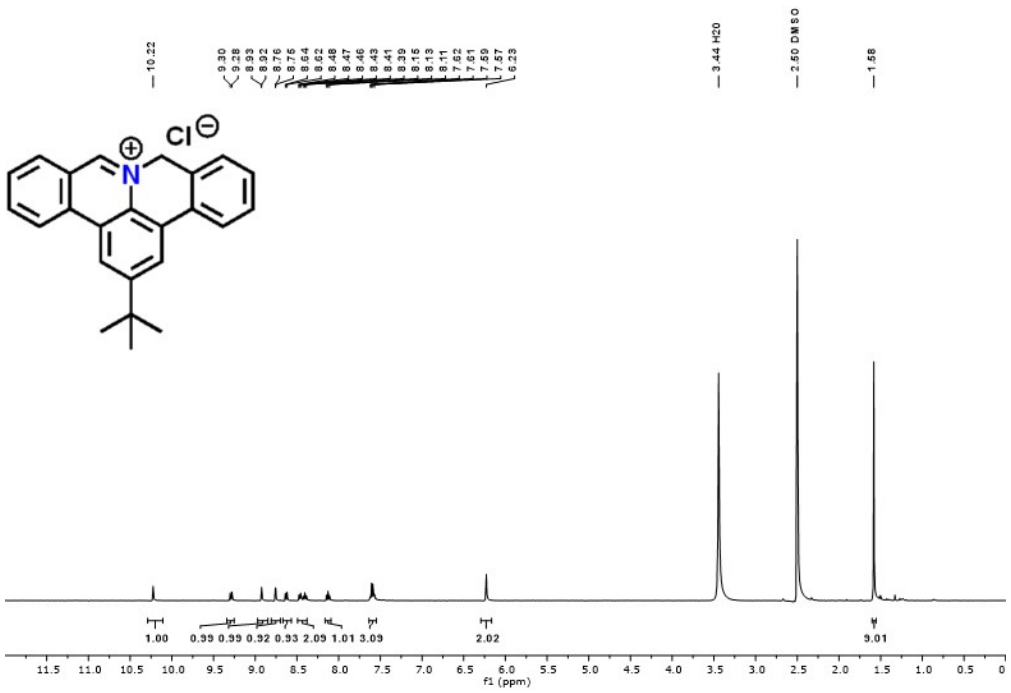

Figure S15. ^{1}H NMR spectrum recorded for **5** (DMSO-d_6).

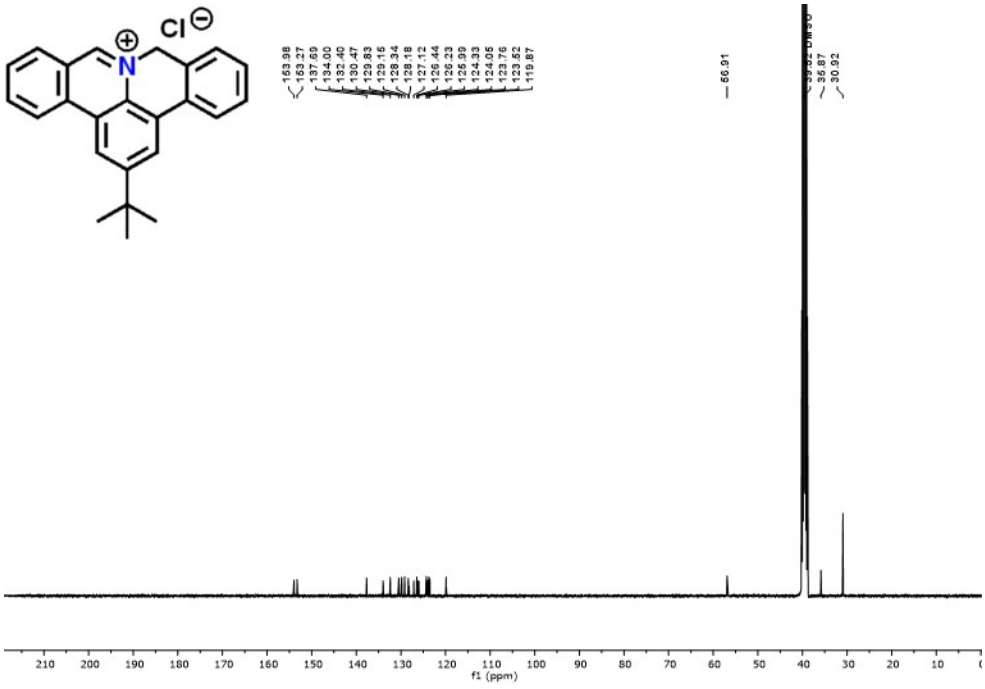

Figure S16. ^{13}C NMR spectrum recorded for **5** (DMSO-d_6).

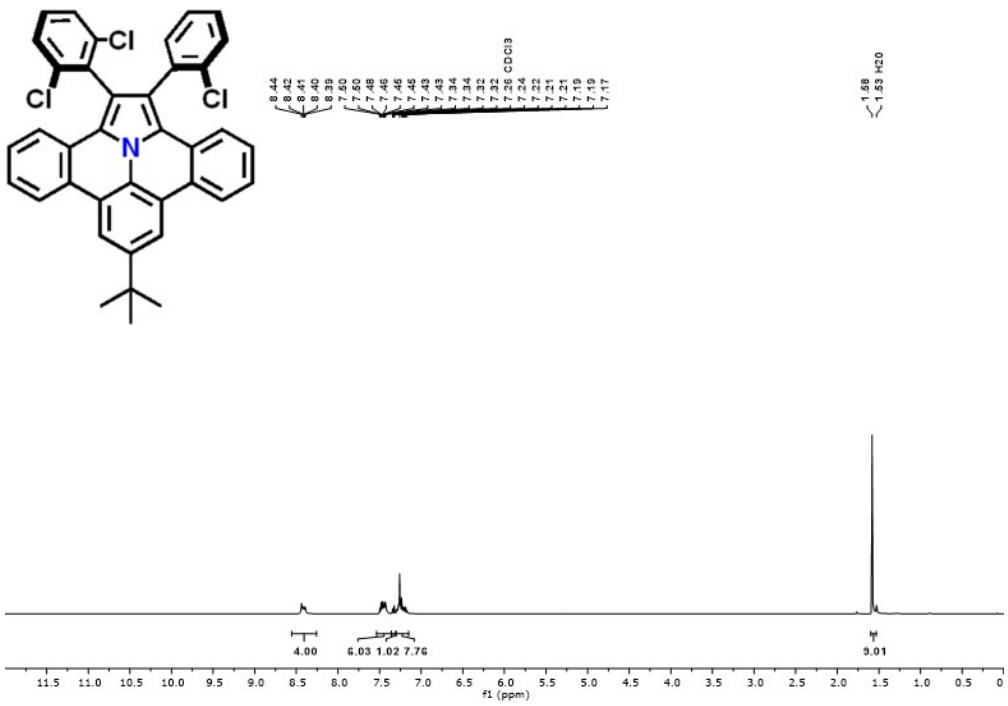

Figure S17. ^{1}H NMR spectrum recorded for **6** ($CDCl_3$).

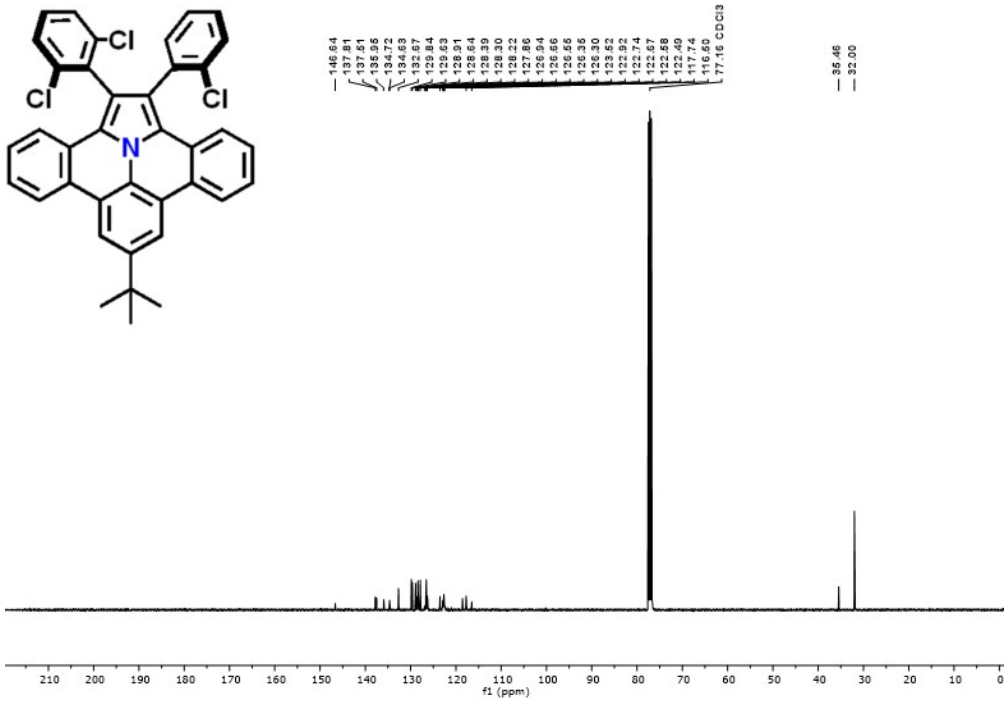

Figure S18. ^{13}C NMR spectrum recorded for **6** ($CDCl_3$).

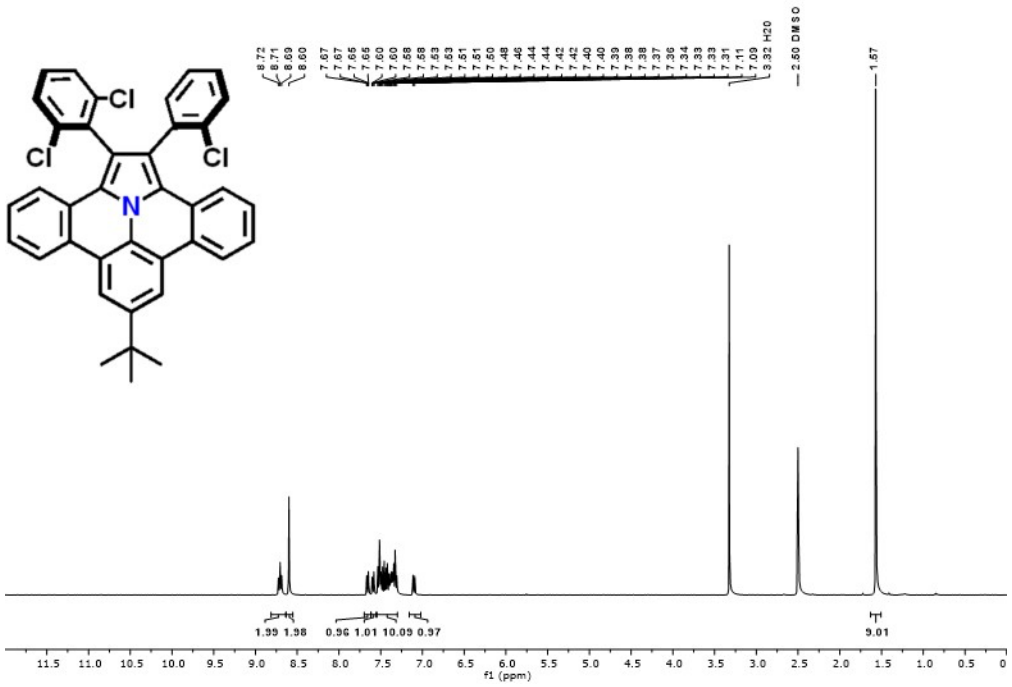

Figure S19. ^{1}H NMR spectrum recorded for **6** (DMSO-d_6).

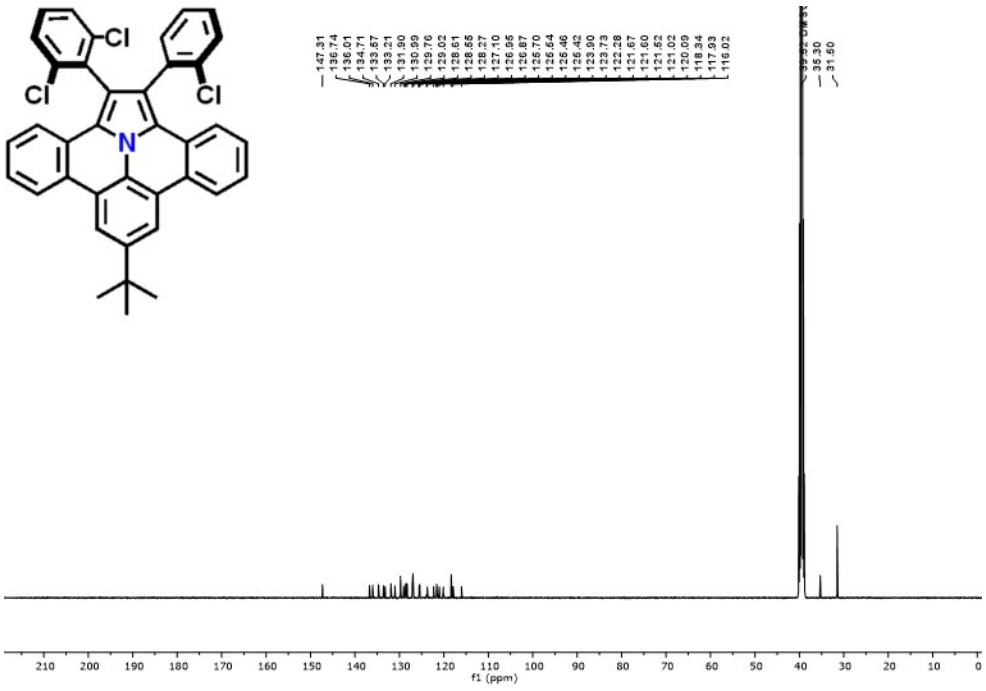

Figure S20. ^{13}C NMR spectrum recorded for **6** (DMSO-d_6).

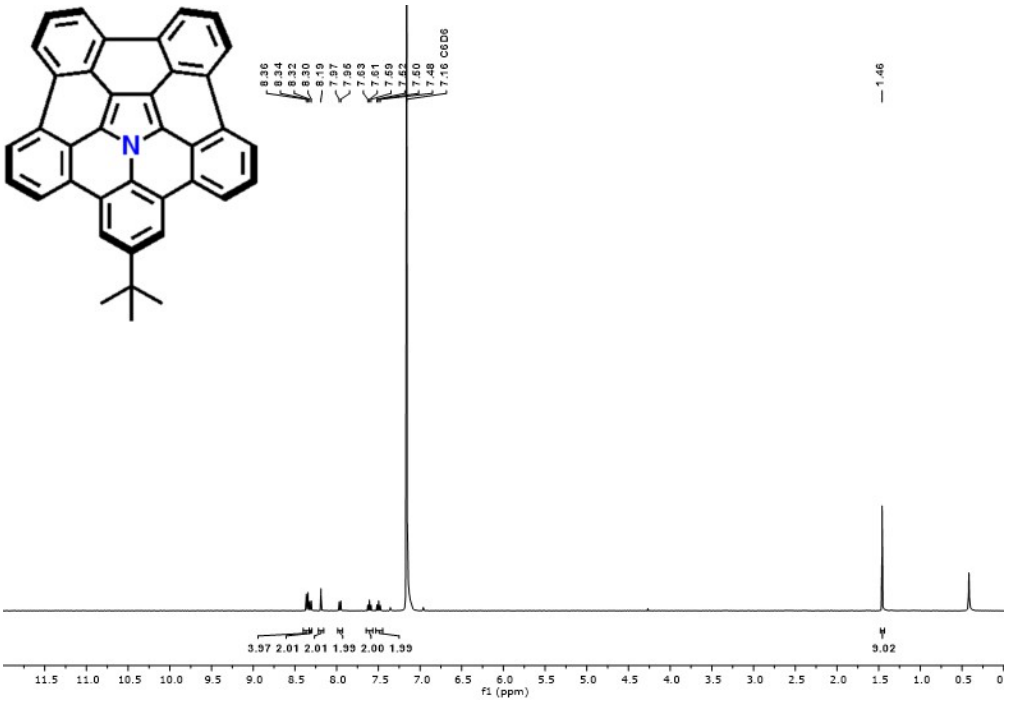

Figure S21. ^{1}H NMR spectrum recorded for **1** (C_6D_6).

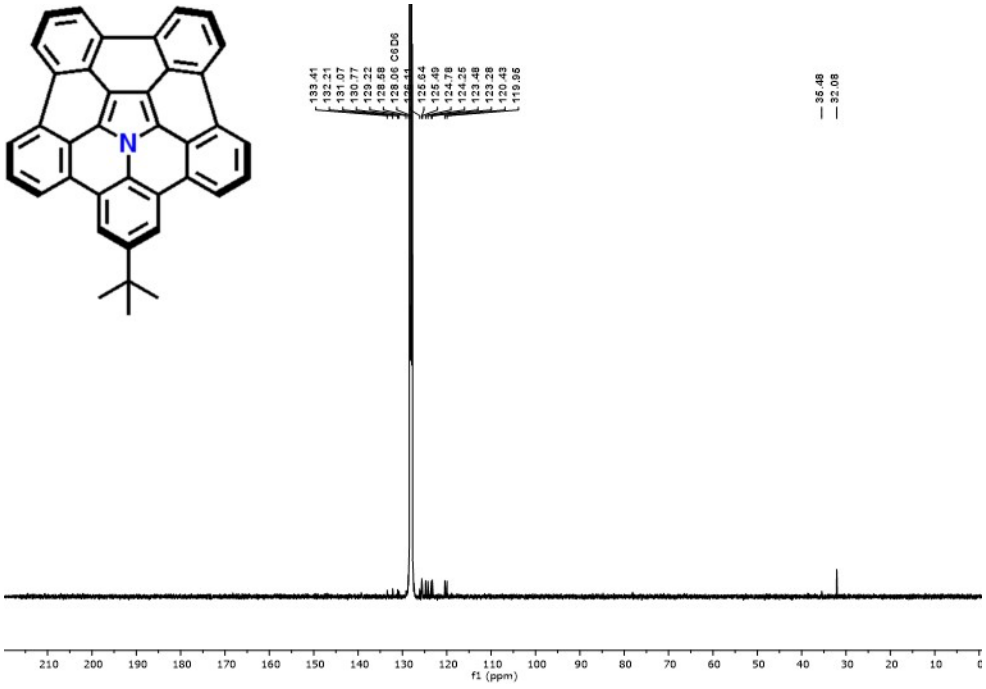

Figure S22. ^{13}C NMR spectrum recorded for **1** (C_6D_6).

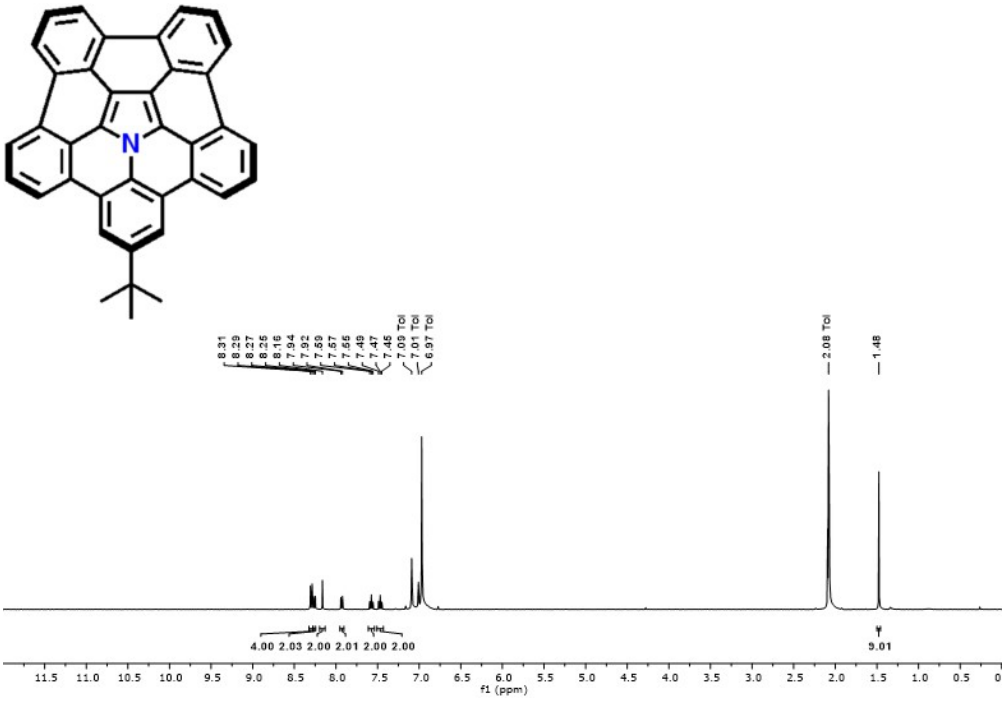

Figure S23. ^{1}H NMR spectrum recorded for **1** (toluene-d_8).

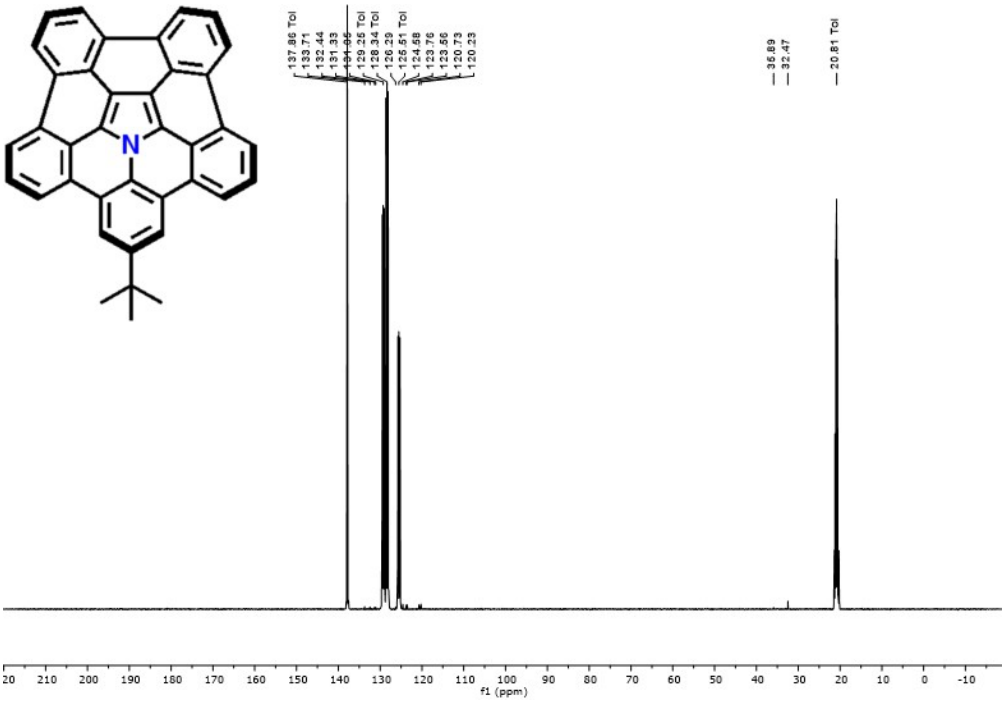

Figure S24. ^{13}C NMR spectrum recorded for **1** (toluene-d_8).

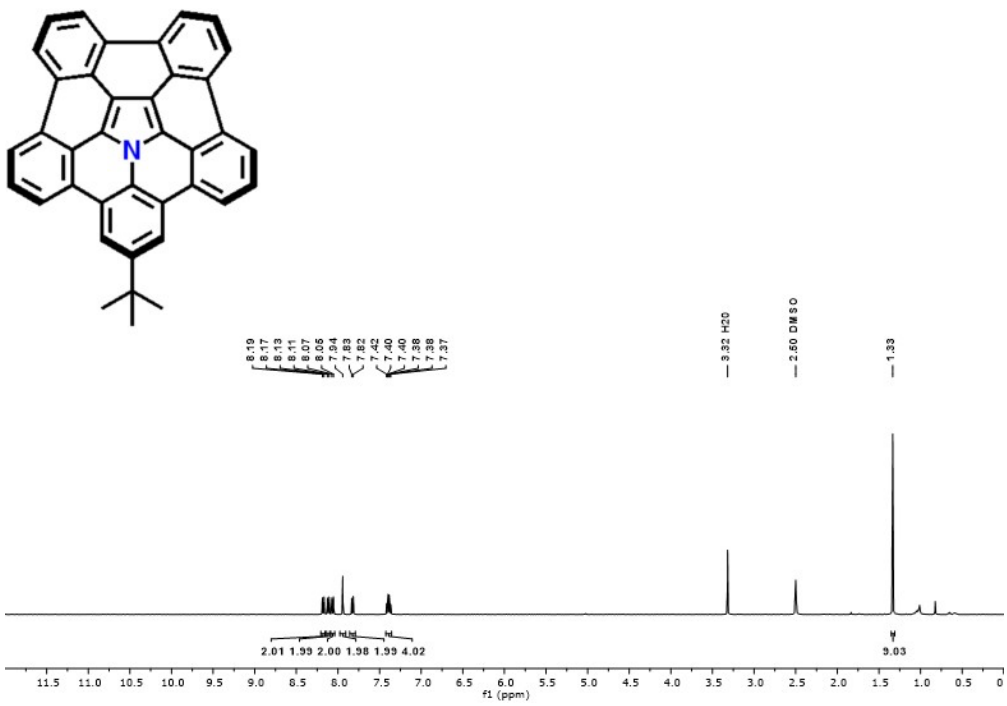

Figure S25. ^{1}H NMR spectrum recorded for **1** (CS_2 with DMSO-d_6 co-axial insert)

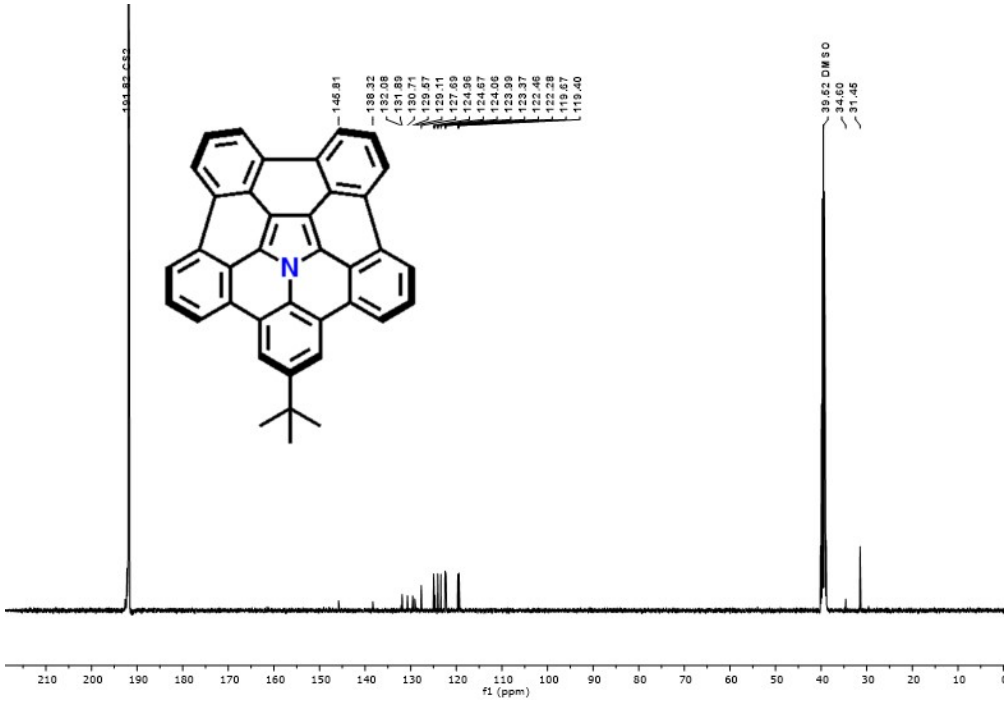

Figure S26. ^{13}C NMR spectrum recorded for **1** (CS_2 with DMSO-d_6 co-axial insert).

Titration Procedures and Data

The titration experiments were performed in accord with literature procedures.[11, 12] In a typical titration experiment, a stock titrand solution of **1** (240 μM) in toluene-d_8 was first prepared and then stirred for 30 min. The titrand solution was used to make a titrant solution of C_{60} (2.5 mM), which was also stirred for 30 min. The titration was then carried out by injecting aliquots of C_{60} via syringe into a 4 mL septum-capped NMR tube loaded with 0.5 mL of the titrand solution. Key metrics are summarized in Table S1. After each addition, the tube was inverted (i.e., flipped up-and-down) 10 times, inserted into an NMR spectrometer, and then analyzed after 12 minutes. The resulting chemical shifts (δ) are reported in ppm and referenced to the residual solvent toluene-d_8, 7.09000 ppm. Three different binding models (e.g., 1:1, 1:2, or 2:1) were used to determine relative stochiometry of the complex formed via the MatLab (BindFit) software package. Host-guest assembly can occur according to Eq. S1 and Eq. S2. Eq. S3 was used to curve-fit the raw data and to obtain the respective association constants. The stepwise association constants (K_1, K_2) can be expressed in terms of the free energy changes (ΔG_1, ΔG_2) according to Eq. S4 and Eq. S5 after correcting for statistical factors. Summaries of the titration data and analyses may be found in Figures S29 – S34 as well as Tables S2 – S8. Fits for data obtained from peaks which resulted in the software program warning that "[t]he Jacobian at the solution is ill-conditioned" were deemed erroneous, and thus not included in the statistical averages presented herein. For the titration conducted at 25 °C this typically included data obtained for peaks 1, 3 and 16 and for every set of peaks (1-16) for the 1 : 2 model (i.e., **1**•$(C_{60})_2$).

$$\boldsymbol{K_1} = \frac{[\mathbf{HG}]}{[\mathbf{H}][\mathbf{G}]} \quad \textbf{(Eq. S1)}$$

$$\boldsymbol{K_2} = \frac{[\mathbf{H_2G}]}{[\mathbf{H}][\mathbf{HG}]} \quad \textbf{(Eq. S2)}$$

$$\Delta\boldsymbol{\delta} = \frac{\boldsymbol{\delta}_{\Delta\mathbf{HG}}[\mathbf{G}]_0\boldsymbol{K_1}[\mathbf{H}]+2\boldsymbol{\delta}_{\Delta\mathbf{H_2G}}[\mathbf{G}]_0\boldsymbol{K_1K_2}[\mathbf{H}]^2}{[\mathbf{H}]_0(\mathbf{1}+\boldsymbol{K_1}[\mathbf{H}]+\boldsymbol{K_1K_2}[\mathbf{H}]^2)} \quad \textbf{(Eq. S3)}$$

$$\Delta G_1 = -R\mathrm{T}\ln\left(\frac{K_1}{2}\right) \quad \textbf{(Eq. S4)}$$

$$\Delta G_2 = -R\mathrm{T}\ln(2K_2) \quad \textbf{(Eq. S5)}$$

The experiments used to create the Job plots were conducted in a similar fashion to the titration experiments described above, with the following exceptions: (1) the combined concentration of **1** and C_{60} was kept constant at 1.0 mM; and (2) separate NMR tubes were used for each data point. Mole fractions were analyzed at every 0.1 increment of added C_{60}, with the exception of 0.33. After each addition, the tube was inverted (i.e., flipped up-and-down) 10 times, inserted into an NMR spectrometer, and then analyzed after 12 minutes. The data shown were obtained by averaging the change in chemical shift of the hydrogen atoms that are defined by peaks 10, 11 and 12 of **1** (see Figure S28).

Table S1. Volumes and quantities used in a typical ^{1}H NMR titration experiment between **1** (240 μM) and C_{60} (2.5 mM) in toluene-d_8 at 25 °C.

Aliquot #	C_{60} Add. Vol. (μL)	Total C_{60} Add. Vol. (μL)	[C_{60}] / [**1**]	C_{60} (mol) / **1** (mol)
1	0	0	0.00	0.00
2	2	2	0.04	0.04
3	3	5	0.09	0.09
4	4	9	0.16	0.17
5	6	15	0.27	0.28
6	7	22	0.39	0.41
7	7	29	0.51	0.54
8	9	38	0.65	0.70
9	9	47	0.80	0.87
10	10	57	0.95	1.06
11	10	67	1.10	1.24
12	14	81	1.29	1.50
13	18	99	1.53	1.83
14	24	123	1.83	2.28
15	30	153	2.18	2.83
16	30	183	2.49	3.39
17	37	220	2.84	4.07
18	42	262	3.20	4.85
19	50	312	3.58	5.78
20	58	370	3.97	6.85
21	67	437	4.35	8.09
22	76	513	4.73	9.50
23	86	599	5.09	11.09
24	96	695	5.44	12.87
25	100	795	5.75	14.72
26	100	895	6.01	16.57
27	150	1045	6.34	19.35
28	250	1295	6.77	23.98
29	500	1795	7.34	33.23
30	1000	2795	7.97	51.75

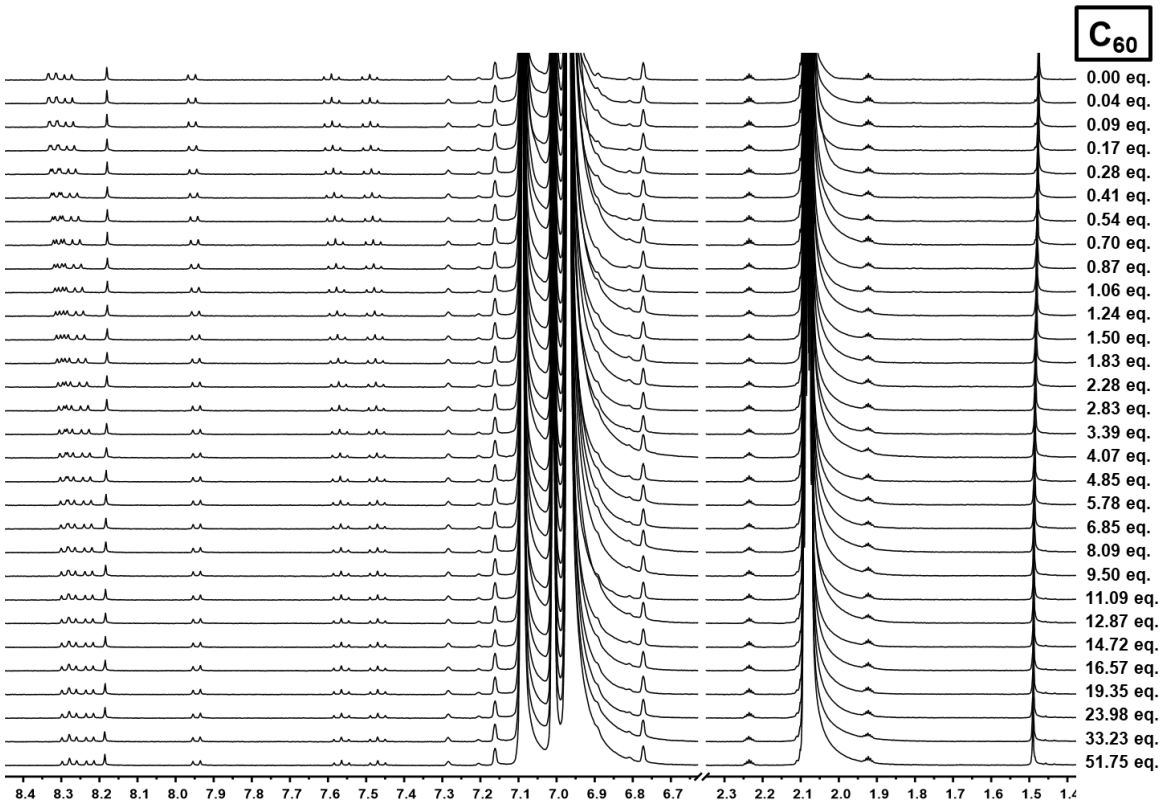

Figure S27. Stacked ^{1}H NMR spectra from a representative titration experiment that was conducted using **1** (240 µM) and 0-52 equivalents of C_{60} (2.5 mM) in toluene-d_8 at 25 °C.

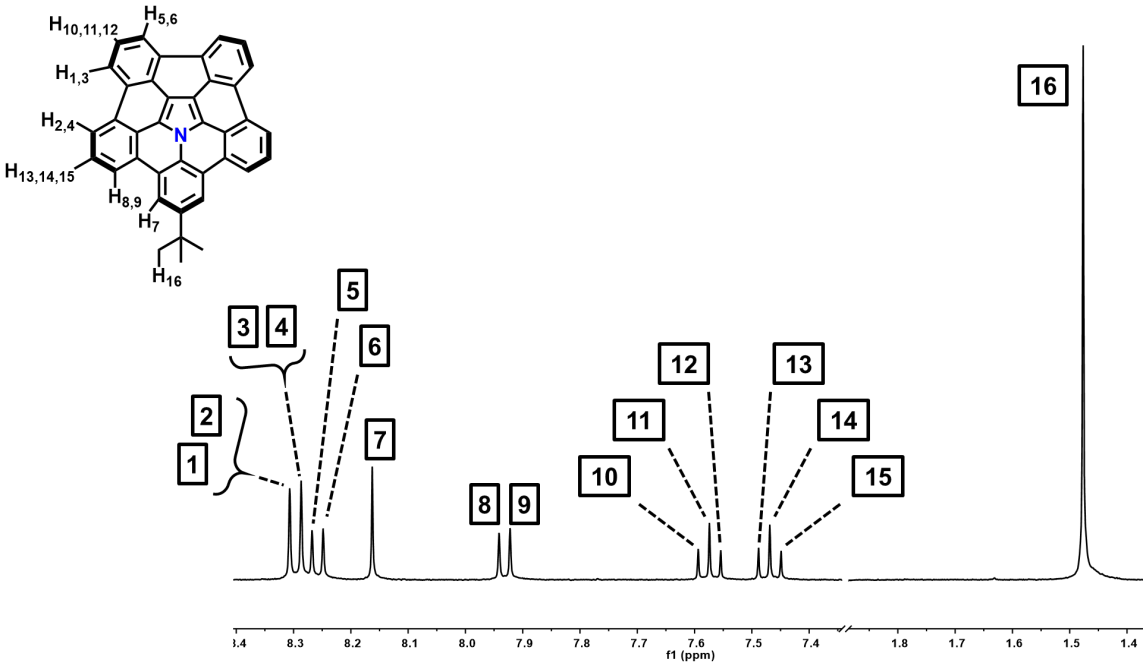

Figure S28. ^{1}H NMR spectrum of **1** (toluene-d_8 at 25 °C) and the corresponding peak assignments that were used in the titration experiments and the nonlinear regression analyses.

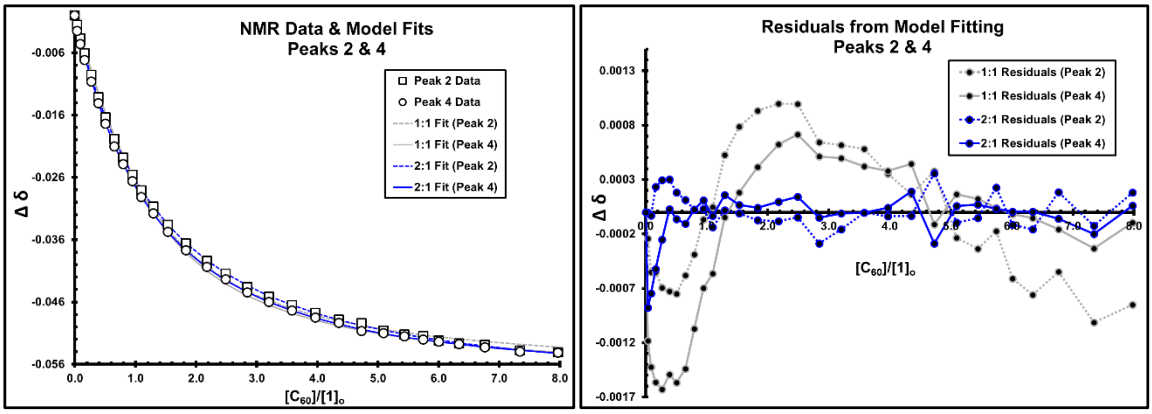

Figure S29. (left) Binding isotherms of two separate models (1:1-gray and 2:1-blue) fitted to the ^{1}H NMR data (circle and square) obtained for peaks 2 & 4 from a titration experiment of **1** (240 µM) with C_{60} (2.5 mM) in toluene-d_8 at 25 °C. (right) The corresponding residual plot from the model fitting process.

Table S2. Results from the nonlinear regression analysis for peaks 2 & 4 from a titration experiment of **1** (240 µM) with C_{60} (2.5 mM) in toluene-d_8 at 25 °C.

Model Fitting Results (Peaks 2 & 4)							
Model	**ss**	**SEy**	**CoF**	**K_1**	**Conf. Int. (%)**	**K_2**	**Conf. Int. (%)**
1 : 1	3.07E-05	7.33E-04	1.52E-03	6412.39	5.6	N. A.	N. A.
2 : 1	2.66E-06	2.22E-04	1.39E-04	1572.86	52.2	1975.92	66.2

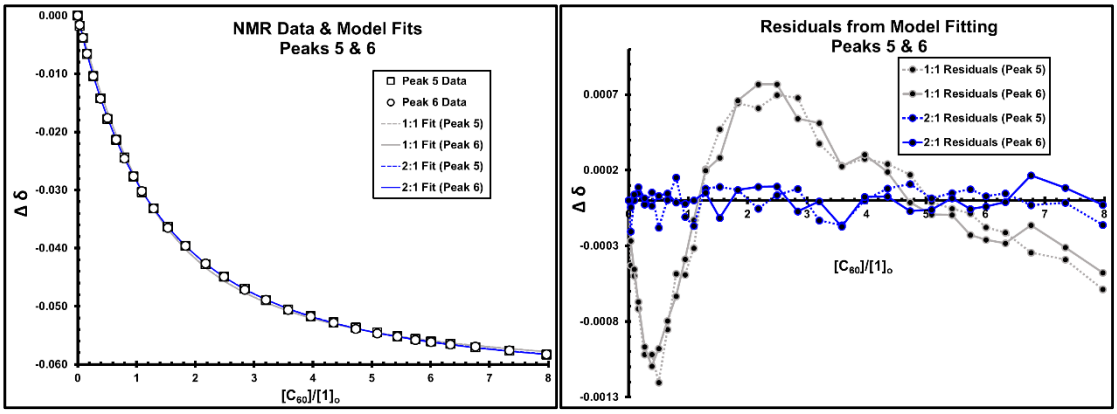

Figure S30. (left) Binding isotherms of 2 separate models (1:1-gray and 2:1-blue) fitted to the ^{1}H NMR data (circle and square) obtained for peaks 5 & 6 from a titration experiment of **1** (240 µM) with C_{60} (2.5 mM) in toluene-d_8 at 25 °C. (right) The corresponding residual plot from the model fitting process.

Table S3. Results from the nonlinear regression analysis for peaks 5 & 6 from a titration experiment of **1** (240 µM) with C_{60} (2.5 mM) in toluene-d_8 at 25 °C.

Model Fitting Results (Peaks 5 & 6)							
Model	**ss**	**SEy**	**CoF**	**K_1**	**Conf. Int. (%)**	**K_2**	**Conf. Int. (%)**
1 : 1	1.68E-05	5.44E-04	7.12E-04	6037.35	3.8	N. A.	N. A.
2 : 1	4.12E-07	8.74E-05	1.86E-05	1793.49	17.4	1143.25	28.1

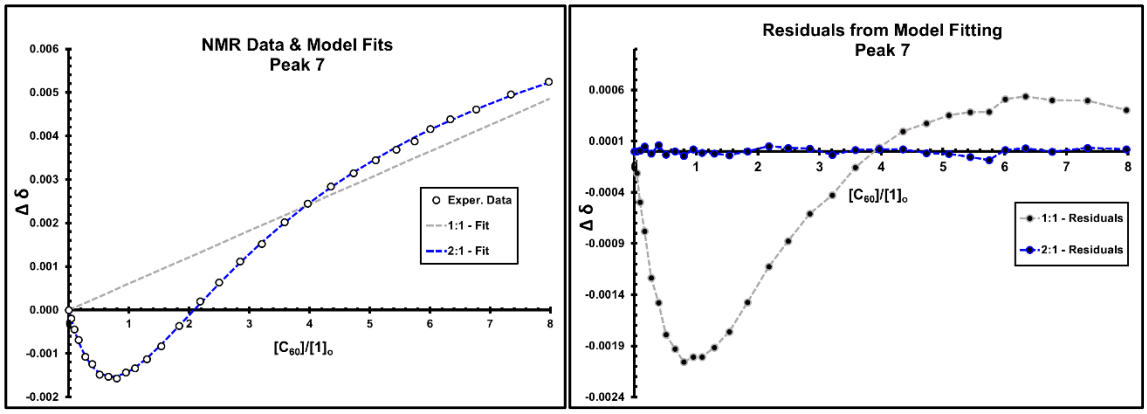

Figure S31. (left) Binding isotherms of 2 separate models (1:1-gray and 2:1-blue) fitted to the ^{1}H NMR data (circle and square) obtained for peak 7 from a titration experiment of **1** (240 µM) with C_{60} (2.5 mM) in toluene-d_8 at 25 °C. (right) The corresponding residual plot from the above model fitting process.

Table S4. Results from the nonlinear regression analysis for peak 7 from a titration experiment of **1** (240 µM) with C_{60} (2.5 mM) in toluene-d_8 at 25 °C.

Model Fitting Results (Peak 7)							
Model	**ss**	**SEy**	**CoF**	**K_1**	**Conf. Int. (%)**	**K_2**	**Conf. Int. (%)**
1 : 1	3.70E-05	1.15E-03	1.64E-01	0.03	494.5	N. A.	N. A.
2 : 1	3.29E-08	3.56E-05	2.08E-04	3131.24	3.6	925.17	45.3

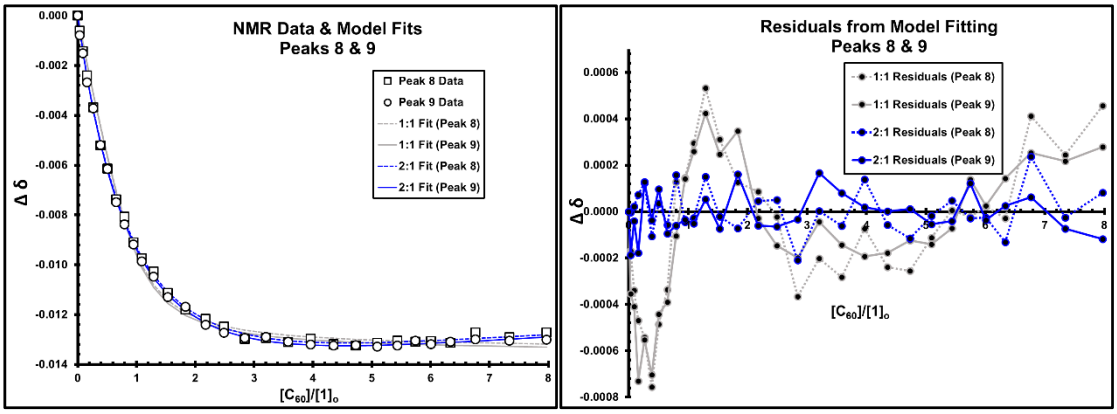

Figure S32. (left) Binding isotherms of 2 separate models (1:1-gray and 2:1-blue) fitted to the ^{1}H NMR data (circle and square) obtained for peaks 8 & 9 from a titration experiment of **1** (240 µM) with C_{60} (2.5 mM) in toluene-d_8 at 25 °C. (right) The corresponding residual plot from the above model fitting process.

Table S5. Results from the nonlinear regression analysis for peaks 8 & 9 from a titration experiment of **1** (240 µM) with C_{60} (2.5 mM) in toluene-d_8 at 25 °C.

Model Fitting Results (Peaks 8 & 9)							
Model	**ss**	**SEy**	**CoF**	**K_1**	**Conf. Int. (%)**	**K_2**	**Conf. Int. (%)**
1 : 1	5.80E-06	3.19E-04	4.97E-03	35904.8	15.9	N. A.	N. A.
2 : 1	4.99E-07	9.61E-05	4.52E-04	2445.49	20.7	1382.06	54.7

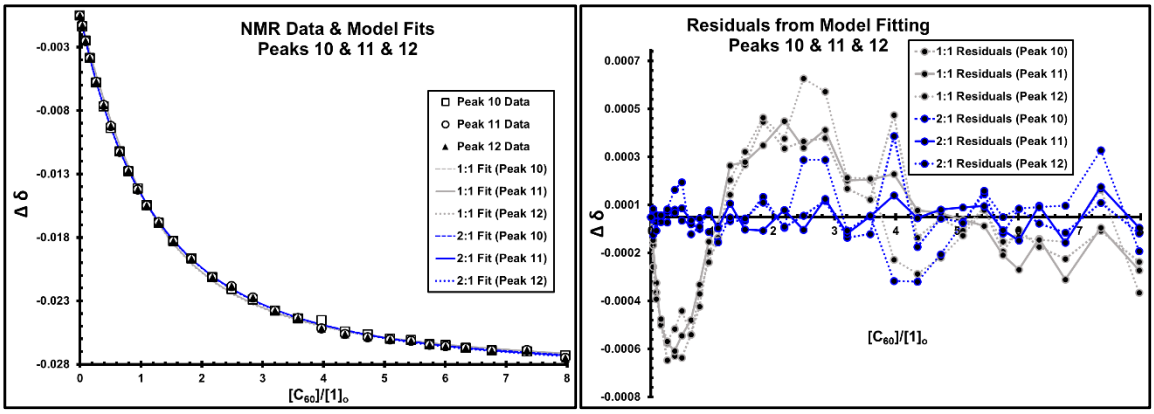

Figure S33. (left) Binding isotherms of 2 separate models (1:1-gray and 2:1-blue) fitted to the ^{1}H NMR data (circle, square and triangle) obtained for peaks 10, 11 & 12 from a titration experiment of **1** (240 µM) with C_{60} (2.5 mM) in toluene-d_8 at 25 °C. (right) The corresponding residual plot from the model fitting process.

Table S6. Results from the nonlinear regression analysis for peaks 10, 11 & 12 from a titration experiment of **1** (240 µM) with C_{60} (2.5 mM) in toluene-d_8 at 25 °C.

Model Fitting Results (Peaks 10, 11 & 12)							
Model	**ss**	**SEy**	**CoF**	**K_1**	**Conf. Int. (%)**	**K_2**	**Conf. Int. (%)**
1 : 1	7.48E-06	2.94E-04	1.00E-03	7799.97	3.8	N. A.	N. A.
2 : 1	7.51E-07	9.57E-05	1.06E-04	2018.53	25.6	1154.79	44.7

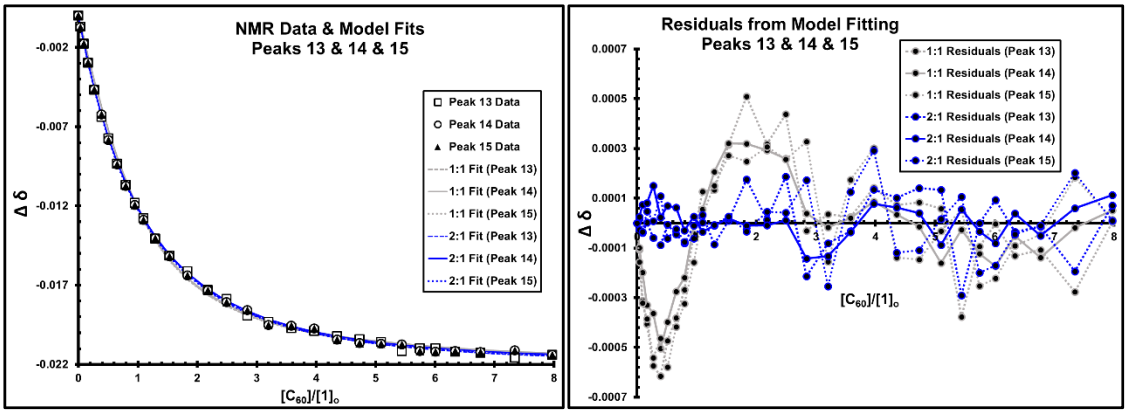

Figure S34. (left) Binding isotherms of 2 separate models (1:1-gray and 2:1-blue) fitted to the ^{1}H NMR data (circle, square and triangle) obtained for peaks 13, 14 & 15 from a titration experiment of **1** (240 µM) with C_{60} (2.5 mM) in toluene-d_8 at 25 °C. (right) The corresponding residual plot from the model fitting process.

Table S7. Results from the nonlinear regression analysis for peaks 13, 14 & 15 from a titration experiment of **1** (240 µM) with C_{60} (2.5 mM) in toluene-d_8 at 25 °C.

Model Fitting Results (Peaks 13, 14 & 15)							
Model	**ss**	**SEy**	**CoF**	**K_1**	**Conf. Int. (%)**	**K_2**	**Conf. Int. (%)**
1 : 1	5.93E-06	2.62E-04	1.24E-03	10603.1	4.5	N. A.	N. A.
2 : 1	8.71E-07	1.03E-04	1.94E-04	2384.46	24.3	934.28	54.6

Table S8. Averaged binding constants, cooperativity and free energy values as obtained from three separate titration experiments between **1** and C_{60}.

Summary of Titration Results						
$[1]_0$	K_1 [a]	K_2 [a]	Cooperativity (α)	ΔG_1 [b]	ΔG_2 [b]	$\Delta\Delta G$ [b]
240 µM	2126 (± 87)	1359 (± 103)	2.56	-4.13	-4.69	-0.56

[a] Units expressed in M^{-1}

[b] Units expressed in kcal mol^{-1}

UV-vis Spectra

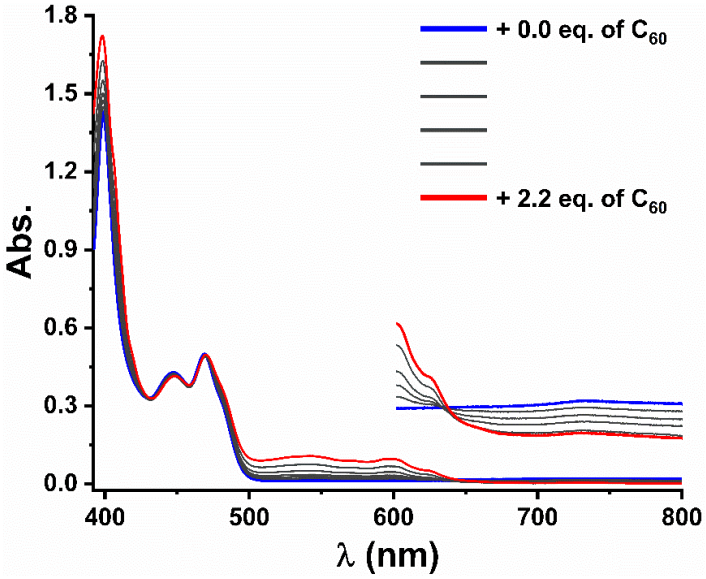

Figure S35. UV-vis spectra as recorded at 25 °C from a toluene solution of **1** (33 µM) that was titrated with up to 2.2 equivalents of C_{60} (1.2 mM). The region from 600-800 nm has been expanded for clarity (see inset).

Diffusion Ordered Spectroscopy (DOSY) Data

Diffusion NMR measurements were conducted in toluene-d_8 at 25 °C and performed using the DgcsteSL_cc pulse sequence without sample spinning. The diffusion delay (Δ) and the diffusion gradient length (δ) were first optimized to achieve a 20% residual signal at 95% gradient strength (compared to an initial gradient strength of 5%) using a 1D DOSY experiment with the DgcsteSL_cc pulse sequence. The gradient pulses were incrementally increased from 5% to 95% which consisted of 16 points. DOSY spectra and data were processed using the OpenVnmrJ 2.1A software. The resulting diffusion coefficients were adjusted to the residual solvent peaks from toluene-d_8.[13]

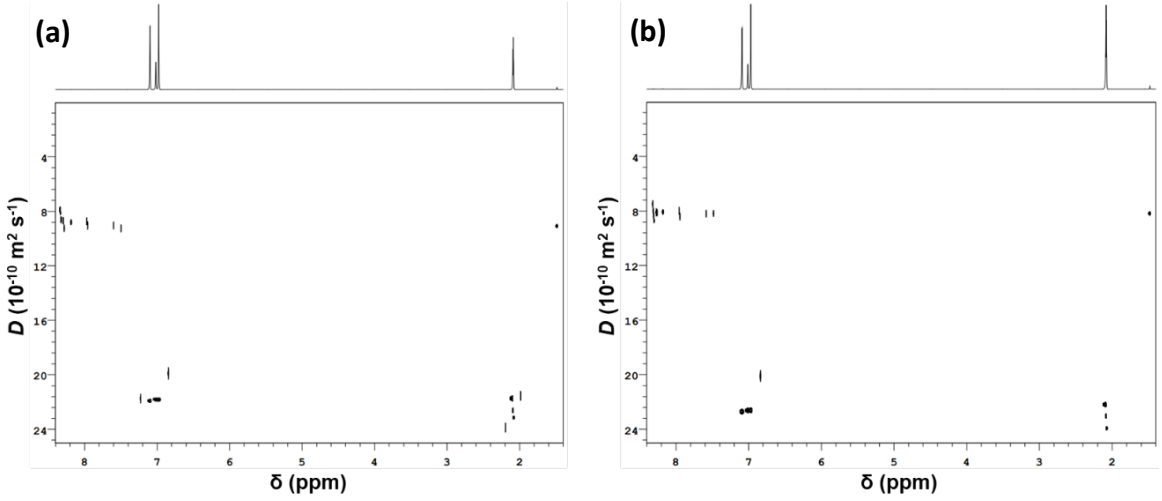

Figure S36. 2D DOSY NMR spectra recorded for (a) **1** (240 μM) and (b) (**1**)$_2$•C_{60} (120 μM) in toluene-d_8 at 25 °C.

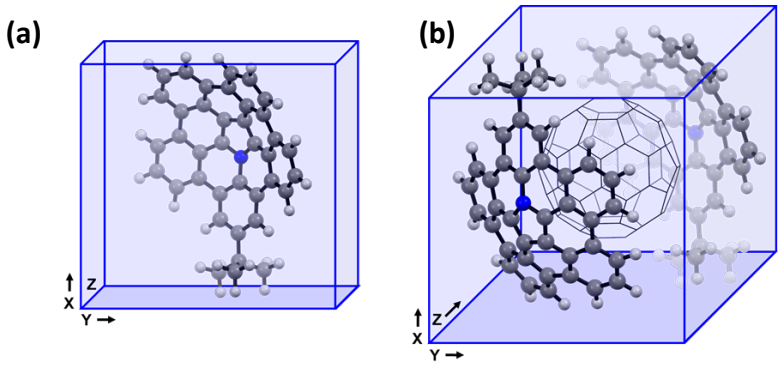

Figure S37. Illustration of the Cartesian-coordinate system that was used for (a) **1** and (b) $(\mathbf{1})_2 \bullet C_{60}$ in the DOSY analysis.

Table S9. Summary of intramolecular distances, radii, and diffusion coefficients.

	1[a]	**1**[b]	$(\mathbf{1})_2 \bullet C_{60}$[c]	$(\mathbf{1})_2 \bullet C_{60}$[b]
x (Å)	**13.385**	**13.577**	**13.350**	**13.502**
y (Å)	**11.108**	**11.364**	**11.055**	**11.269**
z (Å)	**1.880**	**1.994**	**13.769**	**13.472**
$r_{average}$ (Å)	**4.395**	**4.489**	**6.362**	**6.373**
D[d]	**8.77**		**8.14**	
$D_{adjusted}$[d],[e]	**7.43**		**6.54**	
$r_{adjusted}$[f] (Å)	**5.34**		**6.07**	

[a] Crystallographic data obtained from reference [10]
[b] Calculated structures at the M06-2X (6-31G(d,p)) level of theory with dispersion corrections (GD3)
[c] Values obtained from the crystal structure $(\mathbf{1})_2 \bullet C_{60}$
[d] Expressed in units of 10^{-10} m^2 s^{-1}
[e] Diffusion coefficient adjusted to residual solvent peaks from toluene-d_8 according to reference [13]
[f] Calculated according to the Stokes-Einstein equation ($\mathbf{r} = k_b T/6\pi\eta D$), where k_b is the Boltzman constant, **T** is the temperature, η is the viscosity of the liquid (0.00055 Pa s), **r** is the radius, and ***D*** is the diffusion coefficient.

Self-Association Measurements and Data

The self-association constant K, δ_{mon} and δ_{inf} were calculated and optimized as parameters in an isodesmic model (Eq. S6) utilizing a non-linear least-squares curve fit as implemented in the Origin software program, where δ_{mon} and δ_{inf} represent the chemical shifts of the monomer and the infinitely stacked states while δ_{obs} and $[A_o]$ represent the measured chemical shifts and the concentration of **1** or $(\mathbf{1})_2 \bullet C_{60}$, respectively. The ^{1}H NMR data were obtained at 25 °C for **1** and $(\mathbf{1})_2 \bullet C_{60}$ at varying concentrations.

$$\boldsymbol{\delta_{obs}} = \left(\frac{\sqrt{\mathbf{1+4K[Ao]}}-\mathbf{1}}{\mathbf{2K[Ao]}}\right)\boldsymbol{\delta_{mon}} + \left(\mathbf{1} + \frac{\mathbf{1}-\sqrt{\mathbf{1+4K[Ao]}}}{\mathbf{2K[Ao]}}\right)\boldsymbol{\delta_{inf}} \quad \textbf{(Eq. S6)}$$

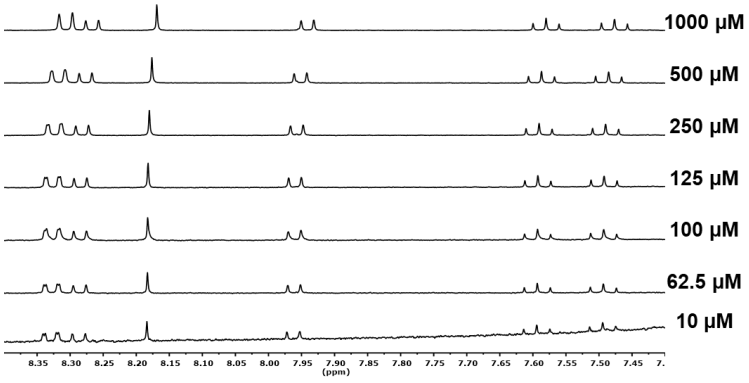

Figure S38. Stacked ^{1}H NMR spectra from a representative serial-dilution experiment that was conducted using **1** (1000 - 10 µM, indicated) in toluene-d_8 at 25 °C.

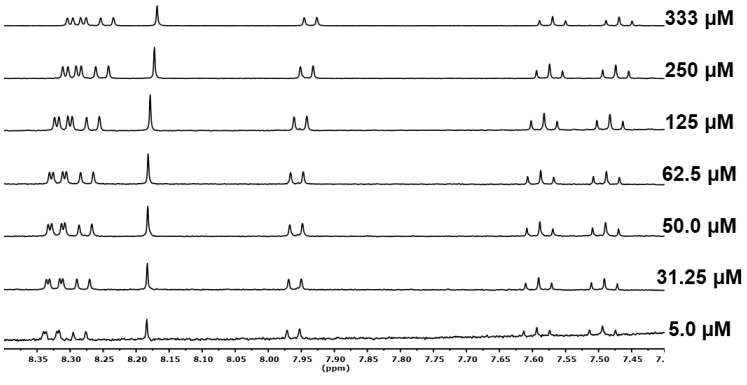

Figure S39. Stacked ^{1}H NMR spectra from a representative serial-dilution experiment that was conducted using $(\mathbf{1})_2 \bullet C_{60}$ (333 - 5 µM, indicated) in toluene-d_8 at 25 °C.

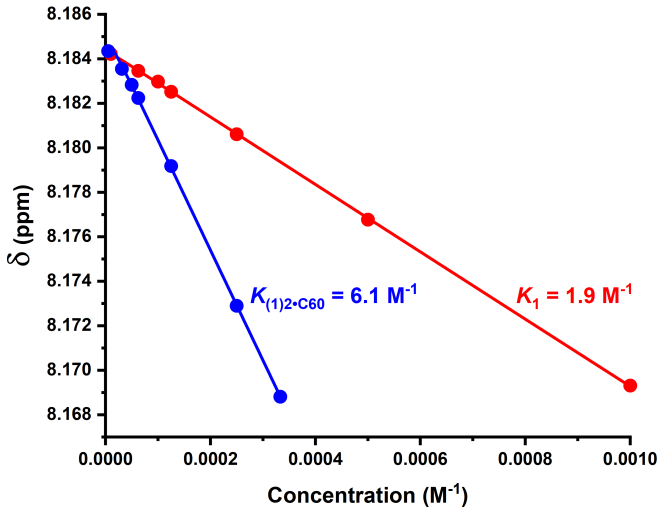

Figure S40. Representative non-linear curve fits of peak 7 for **1** (blue line and circles) and (**1**)$_2$•C$_{60}$ (red line and circles) from serial-dilution experiments that were conducted in toluene-d_8 at 25 °C.

Table S10. Summary of the self-association constants that were calculated from the different hydrogen atoms found in **1** and (**1**)$_2$•C$_{60}$.

Hydrogen	K_1 [a]	$K_{(1)2•C60}$ [a]
$H_{1,3}$	3.0	12.5
$H_{2,4}$	2.5	13.9
$H_{5,6}$	2.4	14.2
H_7	1.9	6.1
$H_{8,9}$	2.7	9.8
$H_{10,11,12}$	1.9	9.1
$H_{13,14,15}$	2.4	9.7
Average (± Std. Dev.)	2.4 (± 0.4)	10.7 (± 2.9)

[a] Units expressed in M^{-1}

Variable Temperature Titration Data

The variable temperature titrations were conducted in a similar fashion as the titration experiments described above and were averaged over two experiments. A narrow temperature range (20 K) was utilized to minimize heat capacity effects.[14] Thermodynamic data were obtained by plotting ln K_a versus T^{-1} (i.e., van't Hoff plots) followed by linear regression. Additionally, a Job plot was conducted in a similar fashion as described above to ascertain the stoichiometry of the complex formed between **1** and C_{60} at 15 °C and 35 °C.

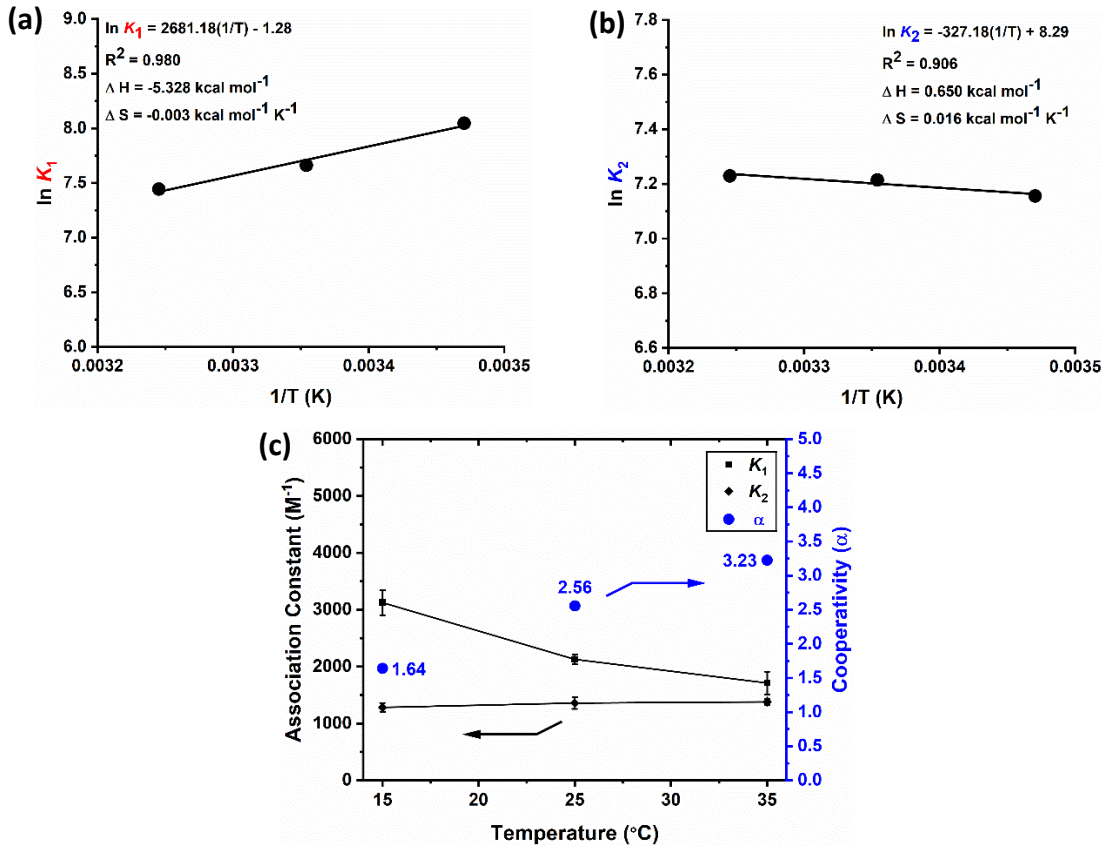

Figure S41. Plots of (a) ln K_1 and (b) ln K_2 versus temperature as obtained from titration experiments that were performed in toluene-d_8 ([**1**]$_0$ = 240 μM) and [C_{60}]$_0$ = 2.5 mM). Linear fits as well as the calculated thermodynamic data are indicated. (c) Plot of association constant values and calculated cooperativity values versus temperature.

Table S11. Averaged binding constant, cooperativity and free energy values as obtained from titration experiments between **1** (240 μM) and C_{60} (2.5 mM) in toluene-d_8 at different temperatures.

Summary of Titration Results						
Temperature (°C)	K_1 [a]	K_2 [a]	**Cooperativity (α)**	ΔG_1 [b]	ΔG_2 [b]	$\Delta\Delta G$ [b]
15	3124 (± 218)	1282 (± 77)	1.64	-4.34	-4.50	-0.16
25	2126 (± 87)	1359 (± 103)	2.56	-4.13	-4.69	-0.56
35	1710 (± 201)	1379 (± 55)	3.23	-4.10	-5.03	-0.94

[a] Units expressed in M^{-1}

[b] Units expressed in kcal mol^{-1}

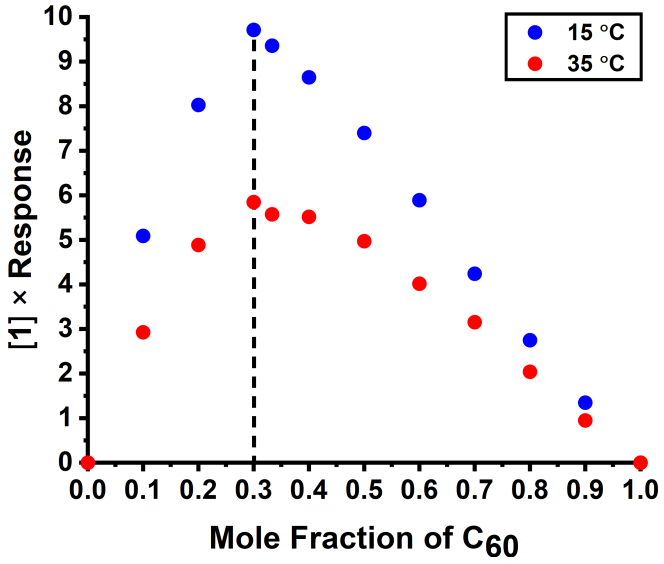

Figure S42. Job Plots that were constructed to ascertain the stoichiometry of the complex formed as obtained by measuring the response, defined as $|\Delta\delta| \times 10^6$, between **1** and C_{60} in toluene-d_8 at 15 °C and 35 °C. See Figure 2b for data that were recorded at 25 °C.

Cyclic Voltammetry Data

Cyclic voltammetry was conducted in a nitrogen-filled glove box with oven-dried glassware using a CH Instruments Electrochemical Workstation (series 680) and a three-electrode configuration, where a platinum disk (diameter: 1.6 mm) was used as a working electrode, a platinum coil was used as a counter electrode and a non-aqueous Ag/Ag+ (acetonitrile, [$AgNO_3$] = 0.01 M, [Bu_4NPF_6] = 0.1 M) was used as a reference electrode. All potentials were determined at a scan rate of 100 $mV \cdot s^{-1}$ and referenced to the ferrocene/ferrocenium redox couple. After each experiment, the disk electrode was polished, and the platinum coil was washed and then flame dried. Data are shown in Figure S43 and are summarized in Table S12.

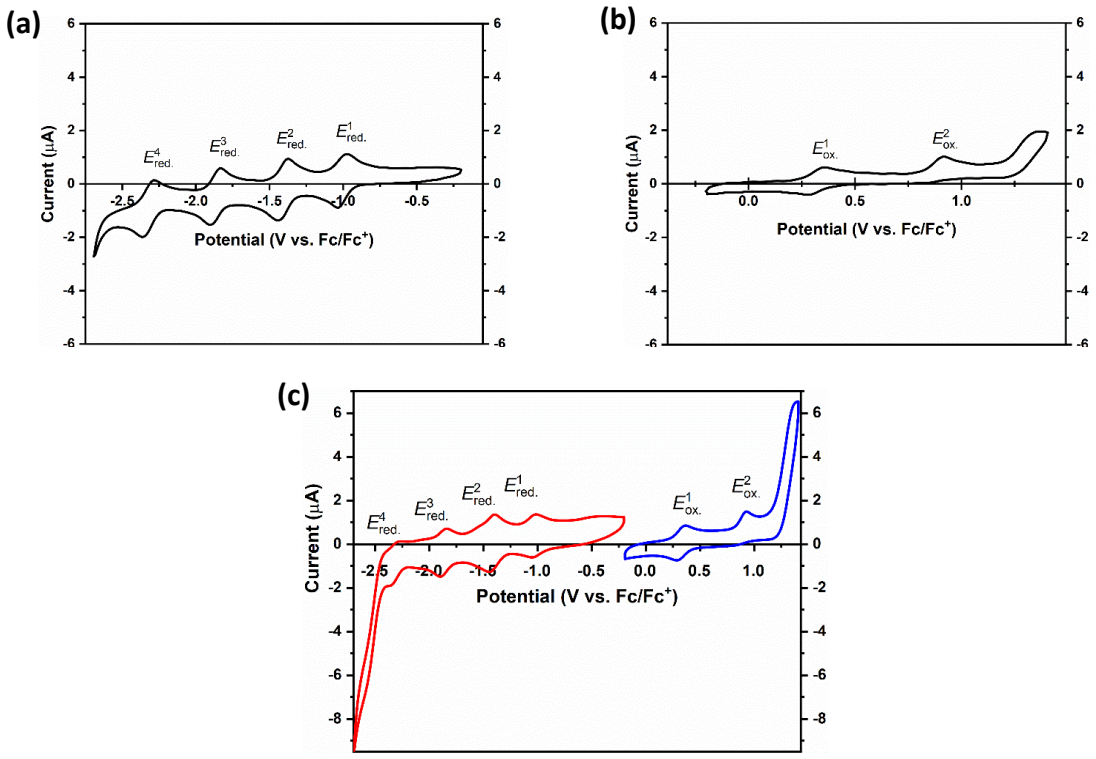

Figure S43. Cyclic voltammograms recorded for solutions of (a) **1** (240 μM), (b) C_{60} (240 μM) or (c) (**1**)$_2$•C_{60} (120 μM) in a mixture of *o*-dichlorobenzene/acetonitrile (5:1 *v*/*v*) that contained Bu_4NPF_6 (0.1 M) as a supporting electrolyte.

Table S12. Summary of oxidation and reduction potential values.

	1	C_{60}	(**1**)$_2$•C_{60}	**Δ**
E_{red}^{1}[a]	-	-1.000	-1.033	-0.033
E_{red}^{2}[a]	-	-1.405	-1.418	-0.013
E_{red}^{3}[a]	-	-1.862	-1.873	-0.011
E_{red}^{4}[a]	-	-2.312	-2.318	-0.006
E_{ox}^{1}[b]	0.355	-	0.367	+0.012
E_{ox}^{2}[b]	0.910	-	0.927	+0.017

[a] Half-wave potential in volts
[b] Peak potential in volts

X-ray Diffraction Data

Compound $(\mathbf{1})_2 \bullet C_{60}$**.** Single metallic, dark-black, block-shaped crystals were obtained by the slow evaporation of a chlorobenzene solution of **1** and C_{60} (2:1 ratio, respectively). X-ray intensity data were collected at 123 K on a Rigaku XtaLAB P200 diffractometer equipped with a Pilatus 200K detector using ω scans and Cu Kα radiation (λ = 1.54187 Å). The images were interpreted and integrated with the program CrystalClear–SM Expert (version 2.1 b45, 2015) from Rigaku.[15] After indexing the X-ray diffraction pattern, the unit cell was refined based on 7843 reflections (19% of the total of 41799 reflections that were measured). Data reduction, scaling and numerical absorption corrections using the ABSCOR program[16] were performed. The final completeness was 97.8% to θ_{max} = 73.585°. Using Olex2,[17] the structure was solved with the ShelXT[18] structure solution program using Direct Methods and refined with the ShelXL[19] refinement package using full-matrix least-squares minimization on F^2. Non-hydrogen atoms were refined anisotropically. Hydrogen atom positions were calculated geometrically and refined in the riding mode. The solvent masking procedure as implemented in Olex2 was used to remove the electronic contribution of chlorobenzene from the refinement, "A solvent mask was calculated and 58 electrons were found in a volume of 275 $Å^3$ in 3 voids per unit cell. This is consistent with the presence of 1 [C_6H_5Cl] per asymmetric unit which account for 58 electrons per unit cell." "Short contacts" were identified with the Platon software.[20] Although solid-state structures which contain C_{60}[21] can exhibit orientation or rotational disorder,[22, 23] twinning,[24] and/or vacancies due to solvent loss,[21] the strong interaction formed between **1** and C_{60} may minimize such defects in the single crystals of $(\mathbf{1})_2 \bullet C_{60}$. Average "ring contacts" were calculated by adding the number of short contacts between **1** and C_{60} and dividing by the number of rings in an identified set (e.g., central, inner, peripheral). CCDC-2115565 contains additional crystallographic data. These data can be obtained free of charge from The Cambridge Crystallographic Data Centre via www.ccdc.cam.ac.uk/structures/.

Crystallographic data of $(\mathbf{1})_2$•C_{60}**:** $C_{136}H_{46}N_2$ (*M* =1707.75 g/mol): triclinic, space group P-1 (no. 2), *a* = 11.11500(10) Å, *b* = 12.5618(2) Å, *c* = 16.5098(2) Å, *α* = 94.2110(10)°, *β* = 108.4190(10)°, *γ* = 111.7000(10)°, *V* = 1984.19(5) Å^3, *Z* = 1, *T* = 123.0 K, μ(Cu Kα) = 0.635 mm^{-1}, *Dcalc* = 1.429 g/cm^3, 41799 reflections measured (5.778° ≤ 2Θ ≤ 147.17°), 7843 unique (R_{int} = 0.0894, R_{sigma} = 0.0362) which were used in all calculations. The final R_1 was 0.0781 (I > 2σ(I)) and wR_2 was 0.2371 (all data).

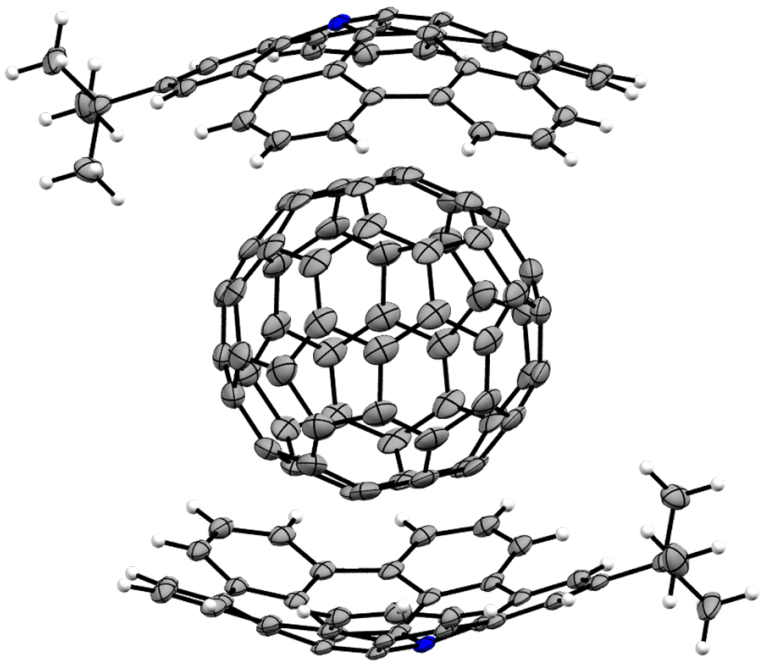

Figure S44. ORTEP diagram of the packing arrangement in the unit cell of crystal structure $(\mathbf{1})_2$•C_{60}. Thermal displacement ellipsoids drawn at the 50% probability level.

Definition of five- and six-membered rings in the symmetric unit (*Cg* indicates the centroid of the ring): Cg1 = N(001)-C(003)-C(004)-C(002)-C(00D); Cg2 = N(001)-C(003)-C(006)-C(00E)-C(00F)-C(005); Cg3 = N(001)-C(005)-C(00Q)-C(00K)-C(00C)-C(00D); Cg4 = C(002)-C(004)-C(007)-C(00B)-C(008)-C(00R); Cg5 = C(002)-C(00D)-C(00C)-C(009)-C(00I)-C(00R); Cg6 = C(003)-C(004)-C(007)-C(00G)-C(00H)-C(006); Cg7 = C(005)-C(00F)-C(00A)-C(00M)-C(00J)-C(00Q); Cg8 = C(006)-C(00E)-C(00L)-C(00T)-C(00O)-C(00H); Cg9 = C(007)-C(00B)-C(00V)-C(00K)-C(00P)-C(00G); Cg10 = C(008)-C(00R)-C(00I)-C(00S)-C(00Z)-C(00U); Cg11 = C(009)-C(00C)-C(00K)-C(00W)-C(010)-C(00N); Cg12 = C(015_a)-C(018_a)-C(01K_a)-

C(01V_a)-C(01A_a); Cg13 = C(01F)-C(01R)-C(01I)-C(016_a)-C(01S_a); Cg14 = C(011_a)-C(013_a)-C(01J_a)-C(01M_a)-C(01A_a)-C(015_a); Cg15 = C(012_a)-C(01K_a)-C(018_a)-C(016_a)-C(01S_a)-C(01O_a); Cg16 = C(017)-C(01D)-C(019)-C(01P)-C(01R)-C(01I); Cg17 = C(017)-C(01I)-C(016_a)-C(018_a)-C(015_a)-C(011_a); Cg18 = C(012)-C(01K)-C(01V)-C(01H)-C(01G)-C(01L); Cg19 = C(01F)-C(01N)-C(01T)-C(01Q)-C(01P)-C(01R).

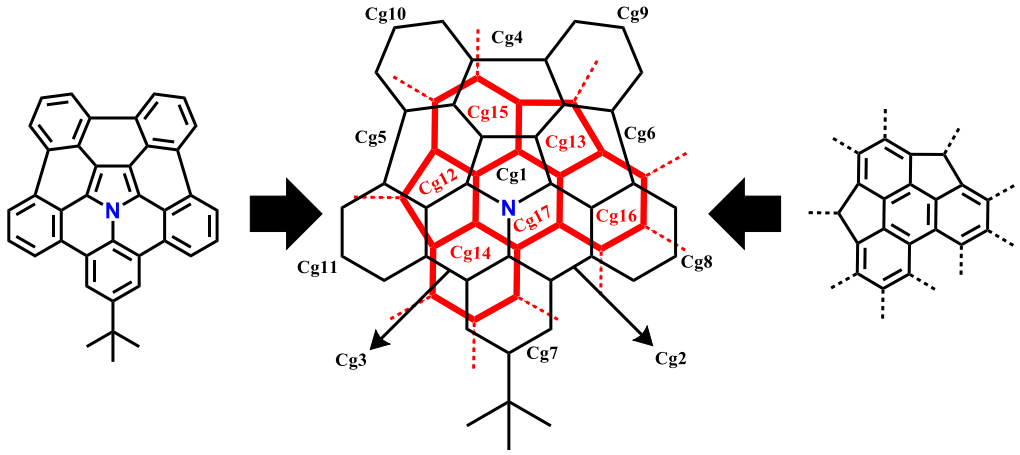

Figure S45. Illustrative guide of the overlap between **1** and the corresponding underlying C_{60} surface as identified by the crystal structure of $(\mathbf{1})_2 \bullet C_{60}$. The double bonds have been omitted in the overlapped structures for clarity.

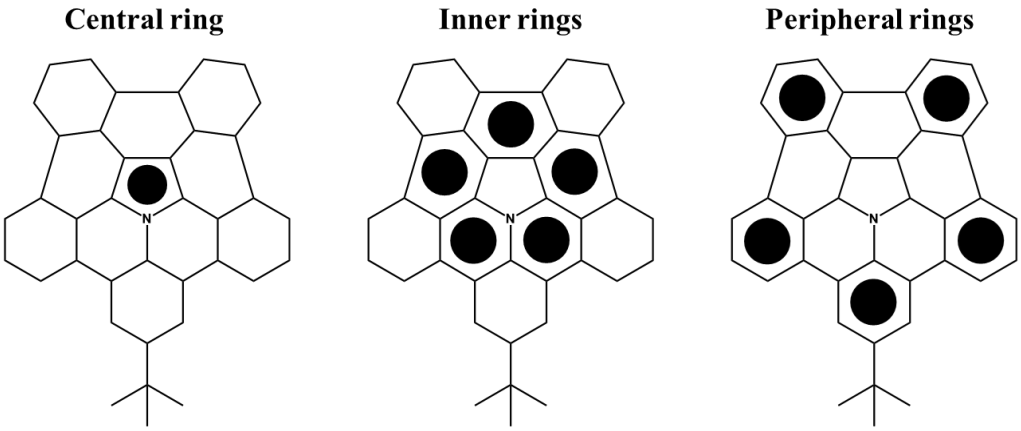

Figure S46. Illustrative guide of the rings on **1**, which are defined by the black circles located in the respective rings.

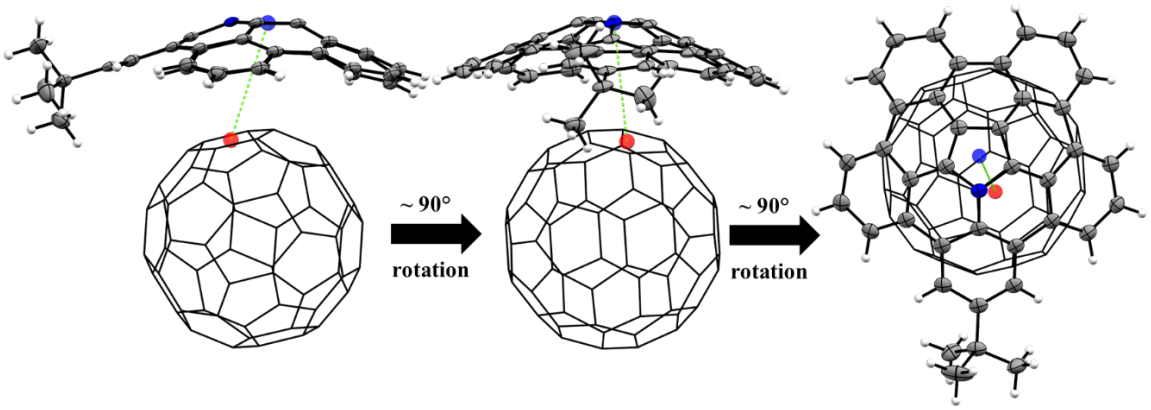

Figure S47. ORTEP diagram of $(\mathbf{1})_2 \bullet C_{60}$ illustrating the ring-to-ring interactions of *Cg1* (central ring) with C_{60}. Thermal displacement ellipsoids drawn at the 50% probability level. A wireframe style was used for C_{60} and the corresponding second molecule of **1** on the bottom half of C_{60} were omitted for clarity. The red and blue spheres represent the centroids on C_{60} and **1** respectively.

Table S13. Geometric data (distances and angles) used to assess the ring-to-ring interactions of ring *Cg1* with C_{60} as identified in the crystal structure of $(\mathbf{1})_2 \bullet C_{60}$.

***Cg(I)*···*Cg(J)*[a]**	***Cg*(centroid)···*Cg*(centroid) (Å)**	**β[b] (°)**	**γ[c] (°)**	***Cg(I)*···J[d] (Å)**	***Cg(J)*···I[e] (Å)**
***Cg1*···*Cg17*[i]**	3.9510(13)	18.3	33.9	3.2800(8)	3.7505(10)

[a] Symmetry codes: (i) x, y, z

[b] Angle ***Cg(I)*** → ***Cg(J)*** vector and normal to plane **I**

[c] Angle ***Cg(I)*** → ***Cg(J)*** vector and normal to plane **J**

[d] Perpendicular distance of ***Cg(I)*** on ring **J**

[e] Perpendicular distance of ***Cg(J)*** on ring **I**

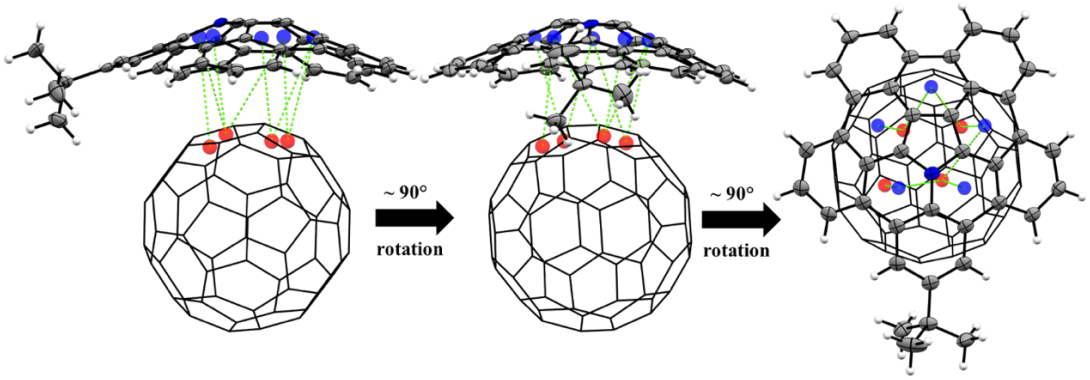

Figure S48. ORTEP diagram of $(\mathbf{1})_2 \bullet C_{60}$ illustrating ring-to-ring interactions of rings *Cg2-Cg6* (inner rings) with C_{60}. Thermal displacement ellipsoids drawn at the 50% probability level. A wireframe style was used for C_{60} and corresponding second molecule of **1** on the bottom half of C_{60} were omitted for clarity. The red and blue spheres represent the centroids on C_{60} and **1**, respectively.

Table S14. Geometric data (distances and angles) for the ring-to-ring interactions of *Cg2-Cg6* with C_{60} that were identified in the crystal structure of $(\mathbf{1})_2 \bullet C_{60}$.

***Cg*···*Cg*[a]**	***Cg*(centroid)···*Cg*(centroid) (Å)**	**β[b] (°)**	**γ[c] (°)**	***Cg(I)*···J[d] (Å)**	***Cg(J)*···I[e] (Å)**
***Cg2*···*Cg17*^{i}**	3.4107(12)	6.8	5.7	3.3941(7)	3.3869(10)
***Cg3*···*Cg12*^{i}**	3.7303(14)	20.6	36.7	2.9927(9)	3.4916(13)
***Cg3*···*Cg17*^{i}**	3.7707(15)	16.2	35.1	3.0856(8)	3.6211(11)
***Cg4*···*Cg13*^{i}**	3.8803(15)	18.9	38.5	3.0350(8)	3.6713(11)
***Cg4*···*Cg15*^{i}**	3.7997(13)	13.6	30.6	3.2689(8)	3.6934(10)
***Cg5*···*Cg15*^{i}**	3.6489(14)	10.2	20.8	3.4112(8)	3.5916(11)
***Cg6*···*Cg13*^{i}**	3.5726(13)	14.7	26.6	3.1934(8)	3.4564(11)
***Cg6*···*Cg17*^{i}**	3.9431(13)	19.2	42.5	2.9085(8)	3.7246(9)

[a] Symmetry codes: (i) x, y, z

[b] Angle ***Cg(I)*** → ***Cg(J)*** vector and normal to plane **I**

[c] Angle ***Cg(I)*** → ***Cg(J)*** vector and normal to plane **J**

[d] Perpendicular distance of ***Cg(I)*** on ring **J**

[e] Perpendicular distance of ***Cg(J)*** on ring **I**

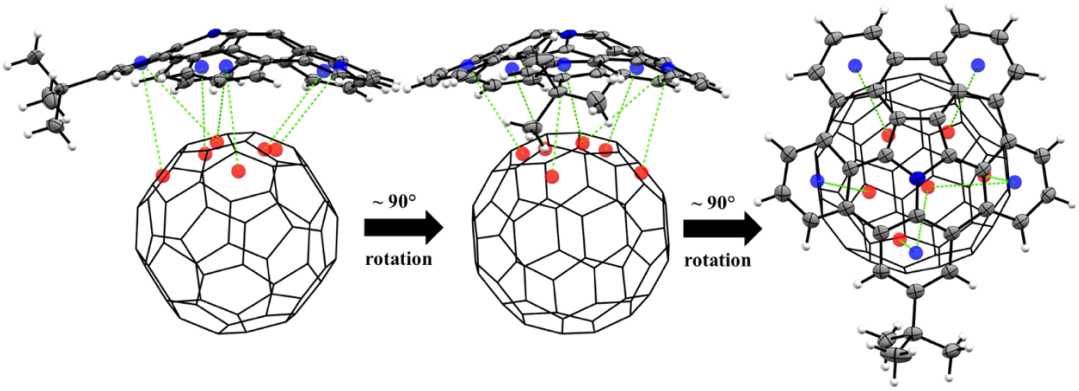

Figure S49. ORTEP diagram of $(\mathbf{1})_2 \bullet C_{60}$ illustrating ring-to-ring interactions of *Cg7-Cg11* (peripheral rings) with C_{60}. Thermal displacement ellipsoids drawn at the 50% probability level. A wireframe style was used for C_{60} and the corresponding second molecule of **1** (which would be located on the opposite side of C_{60}) were omitted for clarity. The red and blue spheres represent the centroids on C_{60} and **1** respectively.

Table S15. Geometric data (distances and angles) for the ring-to-ring interactions of rings *Cg7-Cg11* with C_{60} that were identified in the crystal structure of $(\mathbf{1})_2 \bullet C_{60}$.

***Cg*···*Cg*[a]**	***Cg*(centroid)···*Cg*(centroid) (Å)**	**β[b] (°)**	**γ[c] (°)**	***Cg(I)*···J[d] (Å)**	***Cg(J)*···I[e] (Å)**
***Cg7*···*Cg14*^{i}**	3.9965(13)	10.0	42.9	2.9290(9)	3.9360(11)
***Cg7*···*Cg17*^{i}**	3.7996(15)	24.6	33.5	3.1679(8)	3.4533(11)
***Cg8*···*Cg16*^{i}**	3.7703(12)	9.6	34.6	3.1042(8)	3.7171(9)
***Cg8*···*Cg17*^{i}**	3.9330(13)	25.3	42.3	2.9099(8)	3.5552(9)
***Cg9*···*Cg13*^{i}**	3.6635(15)	18.4	14.4	3.5487(9)	3.4770(11)
***Cg10*···*Cg15*^{i}**	3.7414(13)	16.6	18.0	3.5575(9)	3.5850(10)
***Cg11*···*Cg12*^{i}**	3.5929(16)	13.6	17.6	3.4249(9)	3.4927(13)

[a] Symmetry codes: (i) x, y, z

[b] Angle ***Cg(I)*** → ***Cg(J)*** vector and normal to plane **I**

[c] Angle ***Cg(I)*** → ***Cg(J)*** vector and normal to plane **J**

[d] Perpendicular distance of ***Cg(I)*** on ring **J**

[e] Perpendicular distance of ***Cg(J)*** on ring **I**

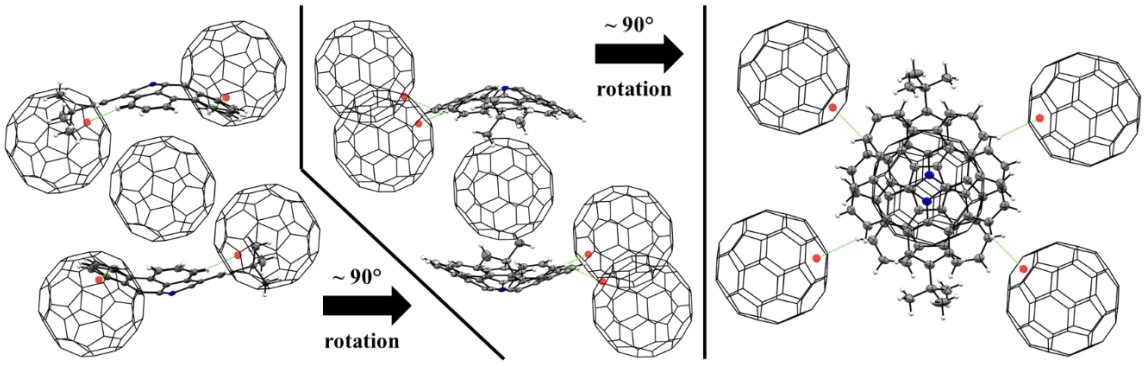

Figure S50. Packing arrangement of $(\mathbf{1})_2 \bullet C_{60}$ showing the linkages to *Cg18* & *Cg19* through intermolecular C–H···π interactions (dotted lines). The red spheres represent the centroids on C_{60}.

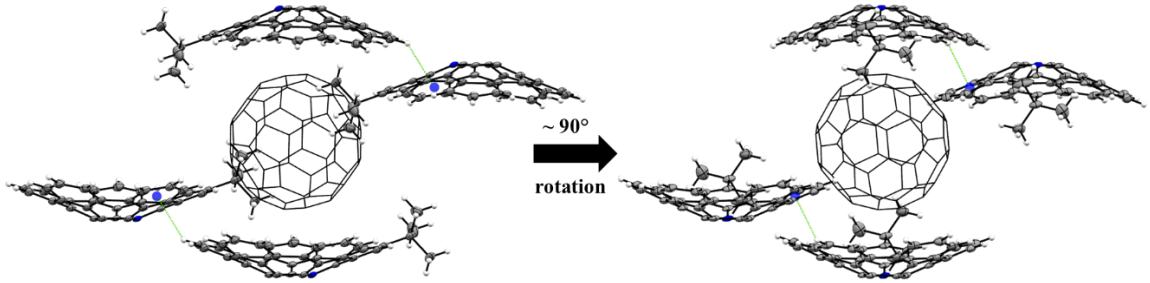

Figure S51. Packing arrangement of $(\mathbf{1})_2 \bullet C_{60}$ showing the linkage of *Cg11* through intermolecular C–H···π interactions (dotted lines). The blue spheres represent the centroids on **1**.

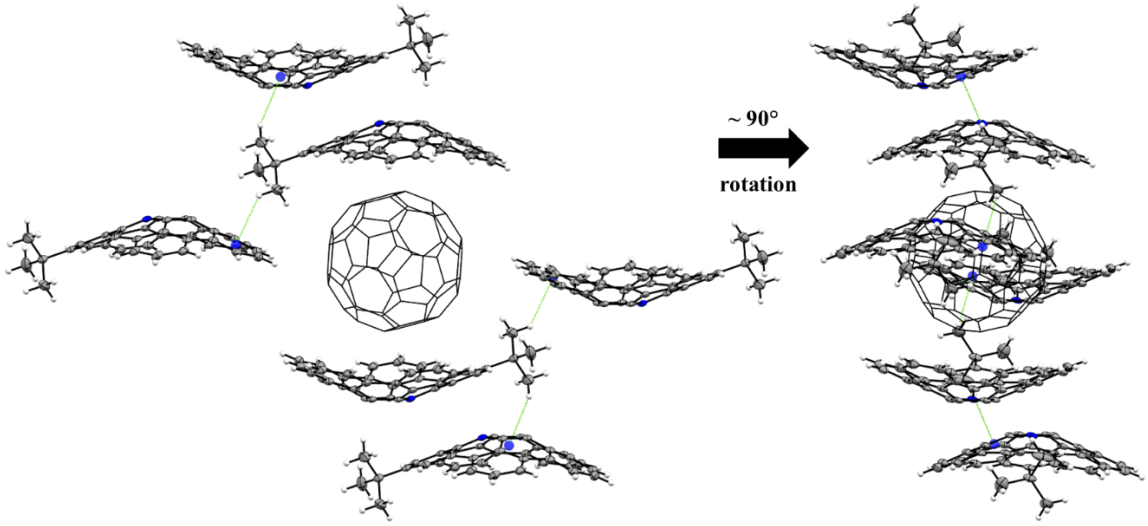

Figure S52. Packing arrangement of $(\mathbf{1})_2 \bullet C_{60}$ showing the linkage of *Cg6* & *Cg10* through intermolecular C–H···π interactions (dotted lines). The blue spheres represent the centroids on **1**.

Table S16. Geometric data (distances and angles) for the hydrogen-to-ring ("C–H···π") interactions that were identified in the crystal structure of $(\mathbf{1})_2 \bullet C_{60}$.

C–H···*Cg*[a]	H···*Cg*(centroid) (Å)	C···*Cg*(centroid) (Å)	C–H···*Cg*(centroid) (°)
C00S–H00S···*Cg18*^{i}	2.99	3.718(3)	135
C00W–H00W···*Cg19*^{ii}	2.88	3.724(3)	149
C00X–H00X ···*Cg11*^{iii}	2.77	3.546(3)	139
C01C–H01C ···*Cg10*^{iv}	2.77	3.464(3)	129
C01X–H01X ···*Cg6*^{v}	2.94	3.854(3)	156
[a] Symmetry code: (i) 1+x, 1+y, z, (ii) 1+x, y, z, (iii) -1+x, y, z, (iv) x, -1+y, z, (v) 1-x, 1-y, -z.			

Geometric Measurements

All binding-induced, stereoelectronic effects were investigated by measuring key distances and angles found in the X-ray and DFT structures using either the Olex2 or Mercury software packages. The bowl-depths, bowl-to-ball (BtB) and intramolecular C_{60} distances were measured first and then utilized in the eccentricity analyses. Finally, POAV along with curvature values were calculated and compared. The following sections are arranged accordingly.

Distance Measurements

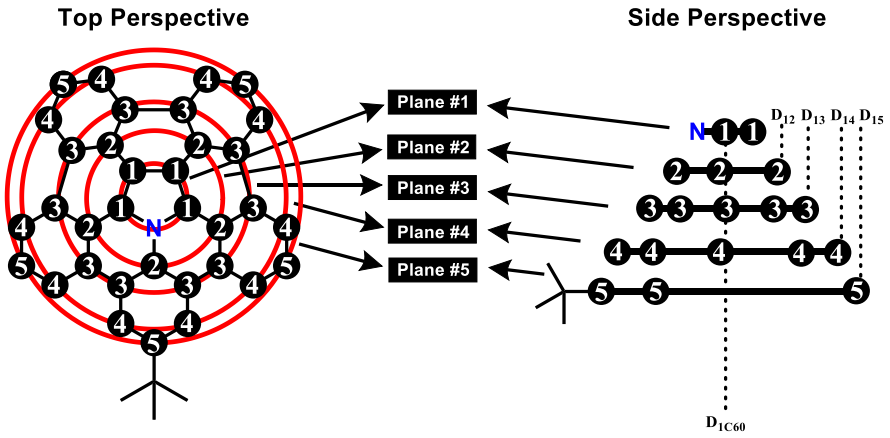

Figure S53. Illustrative guide of the defined planes on **1** and their corresponding centroids used to determine bowl depths and bowl-to-ball (BtB) distances.

Table S17. Summary of bowl depths and bowl-to-ball (BtB) distances that were calculated for complex $(\mathbf{1})_2 \bullet C_{60}$.

Distance Identification[a],[b] **(D_{XY})**	**1**[c] **(Å)**	$(\mathbf{1})_2 \bullet C_{60}$ **(Å)**	Change **(%)**
$\mathbf{D_{12}}$	0.530	0.538	1.51
$\mathbf{D_{13}}$	0.879	0.899	2.28
$\mathbf{D_{14}}$	1.396	1.428	2.29
$\mathbf{D_{15}}$	1.588	1.636	3.02
$\mathbf{D_{1C60}}$	N.A.	6.884	N.A.

[a] D_{XY} is defined as the distance between the centroids of two respective planes, X and Y

[b] Planes were made in Olex2 and are represented by red circles overlapping with numbered carbon atoms in Figure S53

[c] Crystallographic data obtained from reference [10]

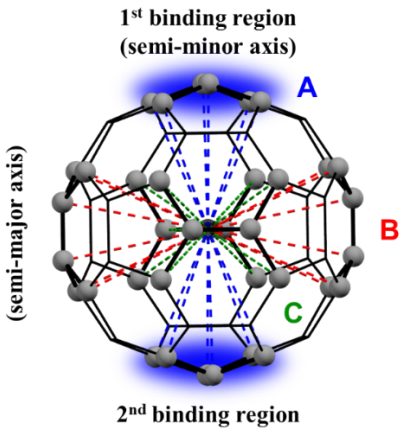

Figure S54. Illustration of the mutually orthogonal intramolecular distances that were calculated for C_{60}.

Table S18. Summary of the intramolecular distances (Å) that were calculated for C_{60} and its associated complexes.

Group[a]	C_{60}[b],[c]	**1**•C_{60}[c]	(**1**)$_2$•C_{60}[c]	(**1**)$_2$•C_{60}[d]
A		7.073 (0.002)	7.068 (0.004)	7.075 (0.007)
B	7.079 (0.001)	7.083 (0.001)	7.086 (0.002)	7.076 (0.004)
C		7.083 (0.001)	7.086 (0.002)	7.075 (0.006)

[a] Each group is composed of six atoms and the resulting distance represents the average with respect to six atom pairs
[b] Value obtained by averaging 15 atom pairs (30 equally distributed atoms) on C_{60}
[c] Calculated structures at M06-2X (6-31G(d,p)) level of theory with dispersion corrections (GD3)
[d] Values obtained from the crystal structure (**1**)$_2$•C_{60}

Eccentricity Measurements

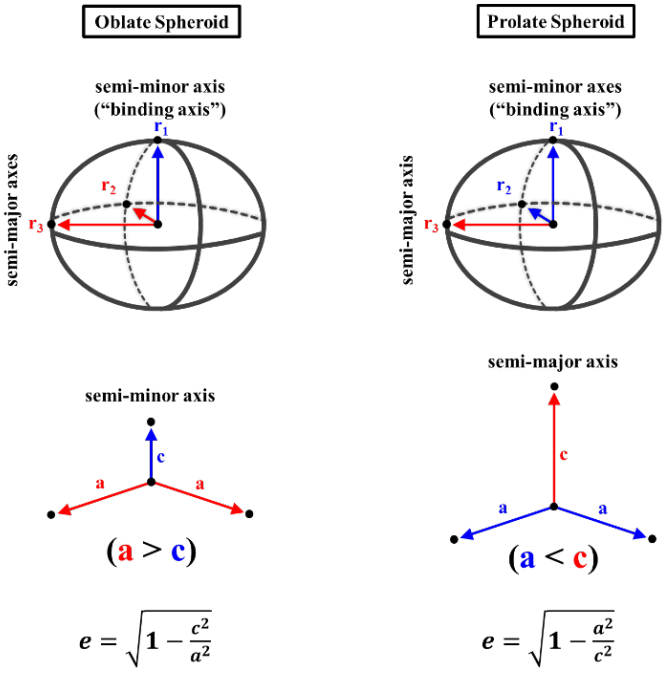

Figure S55. Graphical representation of the mutually orthogonal axes used on C_{60} and its associated complexes to calculate eccentricity for a given spheroid (e.g., oblate or prolate).

Table S19. Summary of the eccentricity values that were calculated for C_{60} and its associated complexes.

Eccentricity	C_{60} [a]	**1**•C_{60} [a]	$(\mathbf{1})_2$•C_{60} [a]	$(\mathbf{1})_2$•C_{60} [b]
e_{12}	0.000	0.053	0.071	0.000
e_{13}	0.000	0.053	0.071	0.024
e_{23}	0.000	0.000	0.000	0.024

[a] Calculated at the M06-2X (6-31G(d,p)) level of theory with dispersion corrections (GD3)
[b] Values obtained from the crystal structure of $(\mathbf{1})_2$•C_{60}

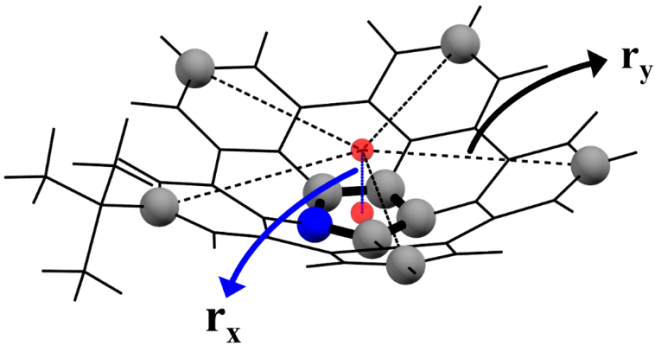

Figure S56. Summary of the metrics that were used to calculate the eccentricity values for **1** or subunits of **1** and are derived from the DFT calculations or the X-ray diffraction data (indicated). Since **1** was treated as an oblate spheroid construct (i.e., two units of **1** were juxtaposed with respect to their concave sides), the radial distances (Å, dotted black lines) from the peripheral atoms to the respective centroid formed by the same atoms were averaged and used as the denominator in the eccentricity equation (see Figure S55). The centroid-centroid distance (Å, dotted blue line) from the pyrrole centroid to the peripheral centroid was used as the numerator.

Table S20. Summary of eccentricity values calculated for **1** and its associated complexes.

Eccentricity	**1** [a]	**1** [b]	**1**•C_{60} [b]	(**1**)$_2$•C_{60} [b]	(**1**)$_2$•C_{60} [c]
e_{xy}	0.948	0.948	0.939	0.939	0.944

[a] Crystallographic data obtained from reference [10]
[b] Calculated at the M06-2X (6-31G(d,p)) level of theory with dispersion correction (GD3)
[c] Values obtained from the crystal structure of (**1**)$_2$•C_{60}

POAV Angle Measurements

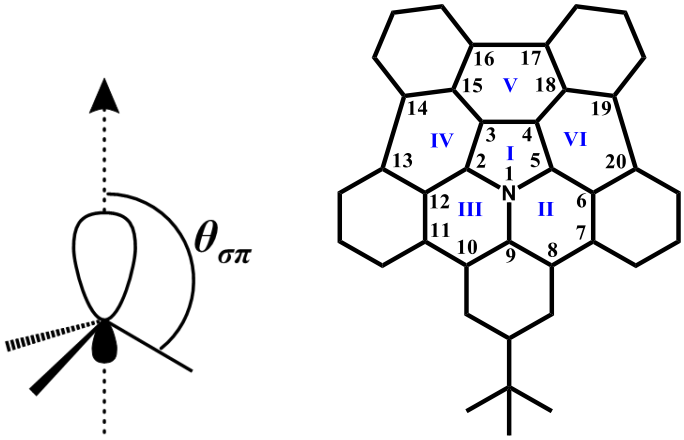

Figure S57. (left) Illustration of a π-orbital axis vector (POAV). (right) Numbering scheme used for **1** in the POAV analysis.

Table S21. Summary of the POAV data for **1** and $(\mathbf{1})_2 \bullet C_{60}$.

Atom	1[a]	$(\mathbf{1})_2 \bullet C_{60}$	Atom	1[a]	$(\mathbf{1})_2 \bullet C_{60}$
1	8.548	8.550	**11**	2.568	2.929
2	7.194	8.064	**12**	3.317	3.526
3	8.937	9.239	**13**	3.145	2.966
4	8.935	8.648	**14**	2.568	3.057
5	7.785	7.348	**15**	3.636	3.711
6	2.771	3.526	**16**	3.148	2.911
7	2.966	3.129	**17**	3.146	2.754
8	2.569	3.004	**18**	3.636	3.301
9	1.483	2.526	**19**	2.344	2.041
10	2.776	3.005	**20**	3.146	2.910

[a] Crystallographic data obtained from reference [10]

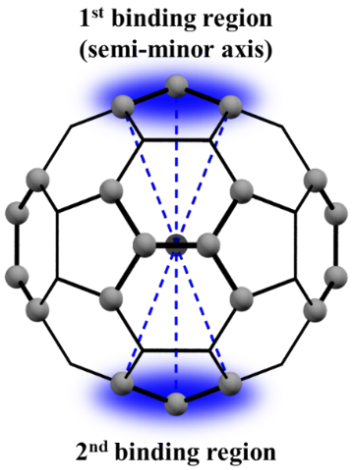

Figure S58. Illustration of the selected atoms on C_{60} that were used in the POAV and curvature analysis calculations.

Table S22. Summary of the POAV values that were calculated for C_{60} and its associated complexes.

Group POAV[a]	C_{60}[b],[c]	**1**•C_{60}[c]	(**1**)$_2$•C_{60}[c]	(**1**)$_2$•C_{60}[d]
1st Binding Region	11.65 (0.02)	11.50 (0.08)	11.55 (0.05)	11.55 (0.13)
2nd Binding Region		11.63 (0.01)	11.55 (0.03)	11.55 (0.13)

[a] Each group (e.g., 1st and 2nd binding region) was averaged over the same 6 atoms used for the intramolecular C_{60} distance analysis
[b] Value obtained by averaging the same 15 atom pairs (e.g., ½ of C_{60} or 30 equally distributed atoms) on C_{60} used for the intramolecular C_{60} distance analysis
[c] Calculated structures at M06-2X (6-31G(d,p)) level of theory with dispersion corrections (GD3)
[d] Values obtained from the crystal structure (**1**)$_2$•C_{60}

Curvature Measurements

Table S23. Summary of curvature values that were calculated for C_{60} and its associated complexes.

Group Curvature[a]	C_{60}[b],[c]	**1**•C_{60}[c]	(**1**)$_2$•C_{60}[c]	(**1**)$_2$•C_{60}[d]
1st Binding Region	0.284	0.279	0.281	0.281
2nd Binding Region		0.282	0.281	0.281

[a] Each group (e.g., 1st and 2nd binding region) was averaged over the same 6 atoms used for the intramolecular C_{60} distance analysis

[b] Value obtained by averaging the same 15 atom pairs (30 equally distributed atoms) on C_{60} used for the intramolecular C_{60} distance analysis

[c] Calculated structures at M06-2X (6-31G(d,p)) level of theory with dispersion corrections (GD3)

[d] Values obtained from the crystal structure (**1**)$_2$•C_{60}

Computational Data

All quantum chemical calculations were performed using the Gaussian 09 software package.[25] The initial geometries for all structures were taken from the crystal structure data. Gas phase geometry optimization and frequency calculations were performed with the Minnesota[26] functional M06-2X and the 6-31G(d,p) basis set.[27-30] Grimme[31]-D3 dispersion corrections were applied as this has been shown to be useful when modeling systems where dispersion forces are operative.[32-36]

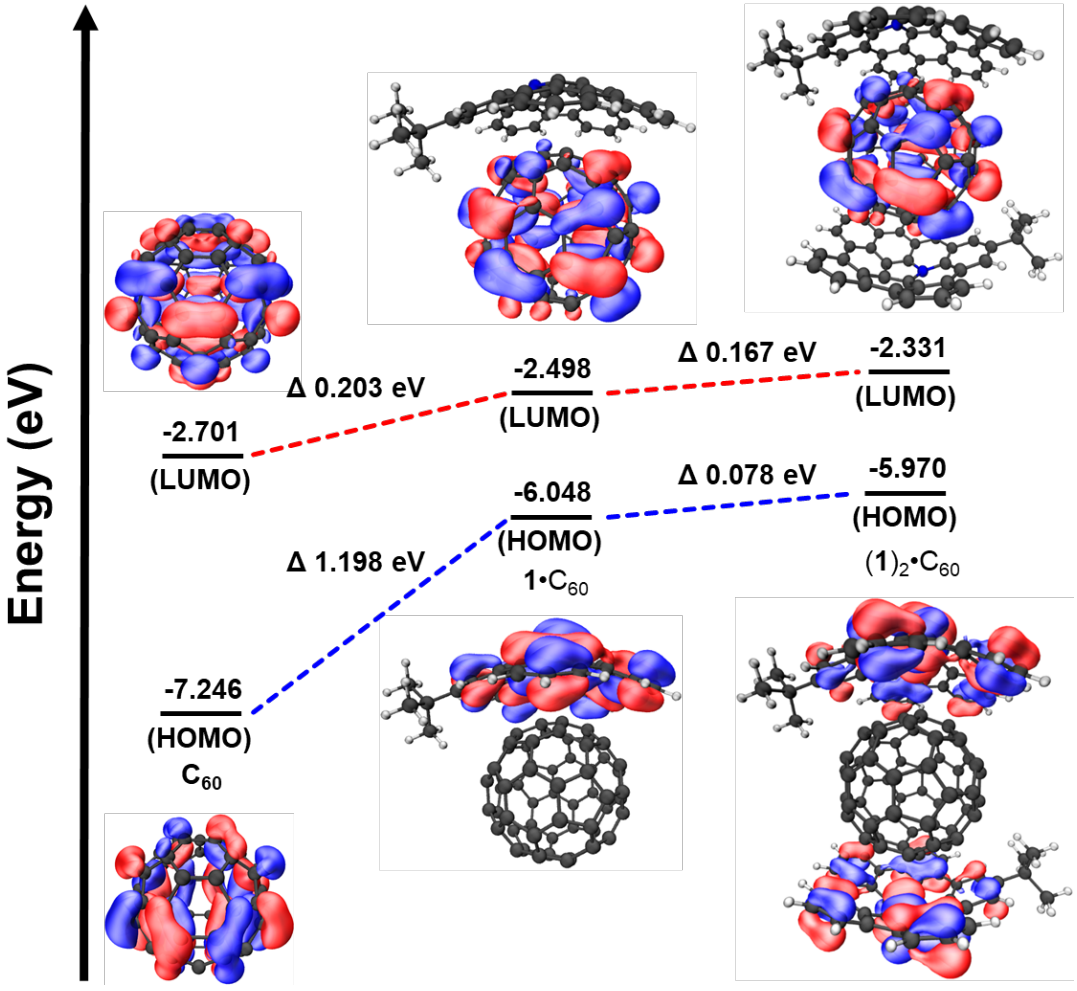

Figure S59. Energy orbital diagrams illustrating the changes in the LUMOs (upper) and the HOMOs (lower) calculated for C_{60}, **1**•C_{60}, and (**1**)$_2$•C_{60}.

1 (M06-2X with GD3 / 6-31G(d,p))

N	-0.2059268065	-0.0612651307	1.1552945246
C	0.5844329783	1.0565860160	1.1382753177
C	1.9088370511	-0.7368029621	1.0154660767
C	0.6037101966	-1.1610304308	1.0557861450
C	1.8964630827	0.6588674349	1.0666100663
C	-2.1195195176	1.2035986357	0.5115042622
C	-1.2704132374	2.4395903482	0.4724786071
C	0.1646945220	-2.3754283026	0.5292974389
C	-3.4664241523	1.1563708308	0.1542696262
H	-3.9962391374	2.0887991787	-0.0166615387
C	-5.6432438924	-0.0082403698	-0.3860359603
C	-1.2286048192	-2.5212344153	0.2899034486
C	-0.6620618662	-4.7240519282	-0.5340957694
H	-0.9963707403	-5.6763925208	-0.9327444764
C	0.1247603912	2.2993064831	0.7022225488
C	2.8917663416	1.4525815620	0.4847647962
C	-1.5125382454	-0.0583292403	0.7380314476
C	4.7884506314	2.9689400526	-0.7186263838
H	5.5623999520	3.5786471953	-1.1737656287
C	4.0560790894	0.7727394792	0.0120604417
C	-4.1526135162	-0.0553010482	-0.0279678441
C	0.6312902834	4.4872346866	-0.0891087760
H	1.3112274268	5.2838015955	-0.3748497338
C	5.0472610785	-1.4948019797	-0.6842194925
H	5.9663696253	-1.0361913088	-1.0362435591
C	2.9168377379	-1.4681178018	0.3766874425
C	-1.6871100621	3.6966927774	0.0425490348
H	-2.7343046903	3.9017637667	-0.1563754302
C	-2.0965099574	-1.3059875345	0.4196280595
C	3.6327084275	-3.4977539774	-0.6539223670
H	3.4950916030	-4.5262979610	-0.9732773280
C	1.1276284189	3.2418701320	0.3233500363
C	-3.4507848842	-1.2611631717	0.0671828717
H	-3.9568803211	-2.1912053198	-0.1622936060
C	2.5502825183	2.8036689364	0.1940697991
C	-1.6244444501	-3.7506849173	-0.2313401448
H	-2.6681679962	-3.9589240518	-0.4445133139
C	0.7073132575	-4.4897038158	-0.4217551402
H	1.3999659046	-5.2513158883	-0.7662308747
C	5.0209454088	1.5940860258	-0.5693627413
H	5.9474804893	1.1784590034	-0.9537568518

C	4.0690828424	-0.7353954822	-0.0438714076
C	-0.7416088525	4.7064678824	-0.1858177987
H	-1.0918254384	5.6799122245	-0.5134282430
C	4.8378972058	-2.8584581161	-0.9356765489
H	5.6215653211	-3.4192441929	-1.4349377538
C	3.5728745142	3.5652192741	-0.3909012527
H	3.4178796715	4.6123554426	-0.6323997735
C	-6.2480684827	-1.4079215359	-0.5371877797
H	-5.7806646288	-1.9643867556	-1.3557357604
H	-7.3148320805	-1.3207893348	-0.7630998299
H	-6.1470386496	-1.9913419314	0.3834053613
C	2.5979638562	-2.7993633174	-0.0139271142
C	1.1830693853	-3.2702710012	0.0818203649
C	-5.8323009358	0.7431025194	-1.7149021749
H	-5.4722909318	1.7738346338	-1.6528288715
H	-6.8940753900	0.7752377025	-1.9810449770
H	-5.2893007258	0.2441621448	-2.5230828586
C	-6.4060749955	0.7262032944	0.7297283279
H	-6.2794130822	0.2134684850	1.6878852509
H	-7.4751365494	0.7620171666	0.4953934261
H	-6.0539111373	1.7546706239	0.8493786426

($\mathbf{1}$)$_2$•C_{60} (M06-2X with GD3 / 6-31G(d,p))

N	3.0645034754	7.1310122272	2.0347234911
C	4.3761701024	8.1278850023	3.8235018523
C	1.9753736841	9.7202440943	4.1507331159
C	5.0700547746	3.5208867640	2.2146778072
C	3.8315597707	3.6076515187	1.5734997234
H	3.3932292025	2.7152103376	1.1439645341
C	0.4332761615	6.2492847200	1.4141318622
C	3.1072041467	4.8046868459	1.5118175184
C	3.7382371132	5.9333948116	2.0816489873
C	0.4827312200	9.3984883847	3.6077880014
C	0.6103651317	10.0473594150	4.4156405213
C	1.0136466928	7.4459229467	2.0903094562
C	0.8721513098	3.7855857267	0.7787574875
H	1.3086798441	2.8058249313	0.6140620962
C	4.2861284683	9.0644803480	4.8971637531
C	3.0459688960	9.8723781828	5.0766859106
C	2.7441227161	10.6056306290	6.2337637546
H	3.4990369996	10.7804562210	6.9938565262
C	5.2493706195	7.0073316013	3.7925130542
C	4.9203286488	5.8799746350	2.8641242048
C	0.3873298640	10.7660847530	5.5897634356
H	0.6168629341	11.0594320285	5.8793583372
C	5.3103107304	8.9713187047	5.8515475706
H	5.3423938992	9.6558455587	6.6930866159
C	1.1684189202	5.1092631840	1.0556009480
H	2.2532609647	5.1227059216	1.0843837851
C	1.8351302982	9.4503376125	3.9450227001
H	2.1916992455	10.1353081744	4.7079561453
C	2.3563392390	7.5595036424	2.4799438453
H	3.0949994256	6.8378790930	2.1451496634
C	1.4496166731	11.0696593967	6.4518273424
H	1.2403349965	11.6269109318	7.3592536224
C	0.5197183092	3.9262137876	0.7105197587
H	1.1180311869	3.0600192394	0.4474745663
C	6.2190833387	6.9609957784	4.7911492684
H	6.9201785421	6.1349153395	4.8519968354
C	6.2660657876	7.9623404995	5.7701727764
H	7.0340889561	7.9068646995	6.5346440498
C	2.7507211368	8.5717597302	3.3517103128
H	-3.7944023506	8.6332543972	3.6423839816
C	5.1389045934	1.0596114894	1.5793963932

H	4.1677042462	0.8530716190	2.0411562616
H	5.7423335404	0.1503057096	1.6532810664
H	4.9837160151	1.2726109310	0.5169515596
C	7.2317831041	2.4122367706	1.6227137775
H	7.1151390607	2.6990778897	0.5732712220
H	7.8135787429	1.4855309330	1.6652832551
H	7.8082707819	3.1955694551	2.1234787700
C	1.2136874946	8.3534861745	2.2512440708
C	1.7438937452	7.2226695182	1.6759476483
C	2.2282978313	8.9544902879	3.0029986755
C	0.9838091228	6.1096502787	1.3068193510
C	3.3563860310	8.1806451185	2.8685957825
C	0.1440923087	8.4596529583	2.5851900299
C	5.5773773574	4.6502532205	2.8742508546
H	6.4930638178	4.5515653541	3.4488568211
C	1.6674071850	4.8797293039	1.1127689521
C	5.8606538500	2.2097719468	2.2886833482
C	6.0562060495	1.8089894995	3.7609511935
H	6.6094975685	2.5660170383	4.3238188633
H	6.6174091147	0.8706100610	3.8227403707
H	5.0892920931	1.6655206455	4.2524949940
N	1.8105958436	1.1601806430	13.2603236610
C	3.1223287055	0.1631193071	11.4717045551
C	0.7215455137	-1.4292801161	11.1445671208
C	3.8161831118	4.7702672857	13.0801470472
C	2.5776638833	4.6835667059	13.7212913919
H	2.1393254417	5.5760427683	14.1507447799
C	1.6871980455	2.0419675912	13.8807289059
C	1.8532949367	3.4865435703	13.7830448047
C	2.4843359038	2.3577879515	13.2133162989
C	1.7365779394	-1.1074843388	11.6874114827
C	0.6434547078	-1.7564301669	10.8796538892
C	2.2675428033	0.8452554440	13.2046530845
C	0.3817811017	4.5057205639	14.5159187499
H	0.0547440294	5.4854974609	14.6805273161
C	3.0323235926	-0.7735891277	10.3981394275
C	1.7921679094	-1.5815027278	10.2186590640
C	1.4903584202	-2.3148766428	9.0616482969
H	2.2452974275	-2.4897786757	8.3015976290
C	3.9955136389	1.2836889256	11.5025950882
C	3.6664482792	2.4111348456	12.4308673563
C	0.8664513040	-2.4752797425	9.7056010526
H	1.8706341835	-2.7686623464	9.4160078467

C	4.0565294983	-0.6805171456	9.4437711355
H	4.0886380178	-1.3651293002	8.6023021947
C	2.4223501692	3.1820230205	14.2391329395
H	3.5071916995	3.1685763888	14.2103308711
C	3.0889708644	-1.1593874943	11.3501593497
H	3.4455214654	-1.8444536606	10.5873030912
C	3.6102251976	0.7316200322	12.8150006664
H	4.3488979038	1.4532806084	13.1496895164
C	0.1958614864	-2.7789362234	8.8435973121
H	0.0133925052	-3.3362854969	7.9362247013
C	1.7736552318	4.3651048222	14.5841140206
H	2.3719734385	5.2313275238	14.8470548910
C	4.9652452542	1.3299344568	10.5039736516
H	5.6663199938	2.1560265830	10.4430453922
C	5.0122666759	0.3284842581	9.5250592993
H	5.7803033597	0.3838940897	8.7605967695
C	4.0045806685	-0.2807470835	11.9433496984
H	5.0482550954	-0.3422843642	11.6526606956
C	3.8850567948	7.2316614603	13.7150966662
H	2.9139087902	7.4382130120	13.2532322878
H	-4.4885484719	8.1409207811	13.6411531021
H	-3.7297686513	7.0187988180	14.7775542329
C	-5.9779068037	5.8789870773	13.6720267878
H	-5.8612414140	5.5923433572	14.7215209673
H	-6.5597288533	6.8056690333	13.6292943460
H	-6.5543795581	5.0955467633	13.1714135414
C	0.0402028711	-0.0623274249	13.0438875212
C	-0.4899797849	1.0685557852	13.6190747576
C	-0.9744339494	-0.6634117059	12.2922326875
C	0.2701152630	2.1816104768	13.9880739263
C	-2.1025153691	0.1104533115	12.4265856999
C	1.3979719439	-0.1685280584	12.7099090720
C	-4.3235193981	3.6408434960	12.4206810771
H	-5.2392274039	3.7394842571	11.8460994473
C	-0.4134844745	3.4115408243	14.1820519558
C	-4.6067944094	6.0813702168	13.0060050223
C	-4.8023710539	6.4819057594	11.5336756687
H	-5.3557510547	5.7248136885	10.9709780610
H	-5.3634873191	7.4203252500	11.4717220790
H	-3.8354510587	6.6251686406	11.0420839568
C	-1.5386528537	1.7156074963	6.2488069255
C	0.8754177265	6.0214766593	4.6636824291
C	2.2063932543	5.9296220613	5.0410241745

C	-2.5388551275	3.7182408985	9.1789792151
C	-1.1558994848	2.4818919372	5.0768979879
C	0.7567508843	0.8384210666	6.3854600782
C	-2.0971073200	6.1675168131	6.6241379969
C	2.8924689884	4.6511455261	4.9808752047
C	0.8471803595	0.7826278775	8.7308168687
C	-2.6470019200	3.7859089495	6.3423030229
C	-2.7184119478	4.9272309533	8.5207983800
C	-0.6041954503	0.9113842846	6.8878931656
C	1.6536552168	0.7573072179	7.5253505443
C	-1.1941795393	4.9131047364	4.7106913214
C	0.1450984542	2.4119417873	4.5962126685
C	-1.8409693514	3.7609093710	5.1346274132
C	2.8764082284	1.4139593636	7.4956817520
C	0.1655779064	4.8379928276	4.2113988391
C	-2.4073899782	2.4876372898	8.4165865980
C	1.2995839946	1.4633812480	9.8519313353
C	-1.4266588702	1.6505952867	9.0811649442
C	-2.7724490616	4.9616555559	7.0696436243
C	-0.5467519620	0.8785617937	8.3365848407
C	2.2170380490	3.5212378578	4.5432643994
C	2.4025672540	2.2574600797	5.2329778916
C	1.1223537236	1.5722356332	5.2660713850
C	0.8202472627	3.6169488135	4.1514814599
C	3.2587687924	2.1807910261	6.3244836676
C	-1.3248601901	6.1433077036	5.4713592074
C	-2.4612908877	2.5205369364	7.0303514998
C	2.7923875713	6.5749743024	9.0458423010
C	0.3783151391	2.2691059460	10.6309624140
C	-0.9526600462	2.3609612590	10.2536240903
C	3.7925871678	4.5723410333	6.1156722621
C	2.4096354484	5.8086901595	10.2177518229
C	0.4969835908	7.4521631657	8.9091875764
C	3.3508417607	2.1230655902	8.6705081523
C	-1.6387367477	3.6394365858	10.3137784193
C	0.4065538519	7.5079535037	6.5638308595
C	3.9007354988	4.5046720048	8.9523454185
C	3.9721480557	3.3633500221	6.7738495344
C	1.8579303005	7.3791977731	8.4067555119
C	-0.3999212512	7.5332763668	7.7692965705
C	2.4479143260	3.3774756732	10.5839571623
C	1.1086375669	5.8786407071	10.6984351652
C	3.0947045949	4.5296718601	10.1600228261

C	-1.6226751714	6.8766242145	7.7989638278
C	1.0881551570	3.4525871183	11.0832473533
C	3.6611230631	5.8029449927	6.8780633216
C	-0.0458500513	6.8272020675	5.4427140849
C	2.6803932186	6.6399883679	6.2134829542
C	4.0261848388	3.3289254318	8.2250045467
C	1.8004849777	7.4120169373	6.9580648625
C	-0.9632997616	4.7693453087	10.7513768036
C	-1.1488317554	6.0331235685	10.0616669811
C	0.1313815694	6.7183474490	10.0285754310
C	0.4334890143	4.6736336409	11.1431645428
C	-2.0050345918	6.1097924647	8.9701619015
C	2.5785939559	2.1472755367	9.8232860140
C	3.7150250500	5.7700448658	8.2642980592

1•C_{60} (M06-2X with GD3 / 6-31G(d,p))

N	4.4831912283	-0.2644114221	0.0626514953
C	3.9330895606	-0.5198362697	-2.2928975194
C	3.2850728384	-3.2125304938	-1.4364827798
C	3.7472711169	3.8042391425	0.0603797052
C	3.8009829199	3.0987734171	1.2651547622
H	3.6239025556	3.6240770439	2.1956069730
C	3.2027007323	-1.4561825727	3.2785234849
C	4.0245549218	1.7166489960	1.3094137552
C	4.2546831217	1.0918214543	0.0631765912
C	2.5937080486	-4.2843409088	0.7570313092
C	2.6312192836	-4.2800203995	-0.7485497264
C	2.8681476236	-2.8318079033	2.8088171571
C	3.3158281211	1.3625256001	3.7461699548
H	3.2552633481	2.4280553349	3.9423751904
C	3.3708916257	-1.4449948309	-3.2234048138
C	3.0207290306	-2.8247169948	-2.7803825141
C	2.2244051079	-3.7118703422	-3.5199772866
H	1.9759435025	-3.5047713882	-4.5560978889
C	3.8902624032	0.8940291649	-2.4253272422
C	4.0785474854	1.7245920420	-1.1942200706
C	1.8485172035	-5.1131328052	-1.5477161450
H	1.3100008235	-5.9510896892	-1.1160988865
C	2.9729571993	-0.8859484334	-4.4469264608
H	2.5548202460	-1.5124013543	-5.2282632213
C	2.7483157296	-0.9011934030	4.4844652851
H	2.2762566667	-1.5269207256	5.2352268942
C	1.7770537339	-5.1256676026	1.5127520135
H	1.2659604311	-5.9647622535	1.0511596977
C	2.0388325086	-3.7250544563	3.5032865896
H	1.7322155320	-3.5195071656	4.5241343392
C	1.6912647681	-4.8466839378	-2.9145315695
H	1.0725232401	-5.5128811765	-3.5070148311
C	2.8453611427	0.4683709798	4.7166122834
H	2.4774455149	0.8660781565	5.6567865951
C	3.4556101810	1.3797120928	-3.6562135496
H	3.3832005250	2.4462296109	-3.8431039945
C	3.0520462858	0.4876896276	-4.6587658846
H	2.7215670490	0.8894561054	-5.6109892666
C	1.5497469885	-4.8653192235	2.8703027434
H	0.9052550604	-5.5363873172	3.4287734118
C	3.3273826813	5.9200746442	1.4069867744

H	2.4697122576	5.4874225443	1.9328503842
H	3.1549737311	6.9966495918	1.3196941236
H	4.2236737744	5.7731255774	2.0180814370
C	4.6717972529	6.0037935679	-0.6897291862
H	5.6033145508	5.8235700369	-0.1446925410
H	4.5037646213	7.0846494728	-0.7393248983
H	4.8031033018	5.6359789274	-1.7114949735
C	4.0102562433	-2.3332028140	0.7448828508
C	4.2680003482	-1.0499196914	1.1667993649
C	4.0415627483	-2.3274656293	-0.6534566980
C	3.8267861948	-0.5310096782	2.3871854229
C	4.3199527286	-1.0427527994	-1.0555815624
C	3.2131535808	-3.2205613434	1.4828666894
C	3.8579214977	3.1004977716	-1.1479765456
H	3.7234610395	3.6402687761	-2.0801601394
C	3.7938125822	0.8817462838	2.5290615916
C	3.4885830710	5.3140558617	0.0093103311
C	2.1944467498	5.5861249987	-0.7766718081
H	2.2514125413	5.2165451964	-1.8043967471
H	2.0002284807	6.6629723446	-0.8190039641
H	1.3415159618	5.1012640146	-0.2922133634
C	-2.9232422832	1.0684745936	3.3616459149
C	1.0115902588	-0.8380056637	0.5807588318
C	1.1743838071	-0.0356546937	-0.5378972798
C	-4.9780370172	-1.4477822540	1.6223198669
C	-1.4973716009	0.8003839920	3.3807688794
C	-2.4962007535	3.0896883908	2.0278323544
C	-1.7168111719	-2.8936592582	1.5977477793
C	0.9918969789	1.4011646360	-0.4338313571
C	-4.4449554832	2.9294826690	0.7267934505
C	-2.6214593923	-1.2558498729	3.1953617880
C	-4.0246260975	-2.4547256137	1.5704124143
C	-3.4120144003	2.1877759870	2.7022605902
C	-3.1343680146	3.5480804142	0.8068914555
C	-0.2578818831	-1.1459689405	2.5318509591
C	-0.6217621176	1.6627273400	2.7349928080
C	-1.3103212379	-0.6363300998	3.2781207966
C	-2.3811834686	3.7285141757	-0.3443630364
C	0.6542372151	-0.2428957657	1.8560111041
C	-4.7694643135	-0.2953866208	2.4799009414
C	-4.9441272722	2.5186851020	-0.5008562754
C	-5.2797143486	0.8752955097	1.7896474667
C	-2.8199841775	-2.3569108725	2.3743449126

C	-4.6161349191	2.0890009782	1.8982412690
C	0.6561243576	1.9713252389	0.7856803401
C	-0.3436109266	3.0226730535	0.8390594975
C	-1.1327856161	2.8322757023	2.0432468789
C	0.4812082668	1.1289355284	1.9573783485
C	-0.9548498803	3.4605377818	-0.3285906104
C	-0.4657568052	-2.2987763044	1.6731630399
C	-3.6178044792	-0.2015907264	3.2481245014
C	-1.6955303022	-0.6589973317	-3.3959315348
C	-5.6384001960	1.2488860454	-0.6140078364
C	-5.8018783359	0.4460247296	0.5051794018
C	0.3589746946	1.8602174852	-1.6558602986
C	-3.1215069536	-0.3903884703	-3.4100451093
C	-2.1246909701	-2.6813144662	-2.0605009901
C	-2.9037339992	3.3000471651	-1.6292245622
C	-5.6158088041	-0.9897142350	0.4015512693
C	-0.1777010419	-2.5202333796	-0.7595086204
C	-1.9983879135	1.6652165957	-3.2263357363
C	-0.5939594764	2.8682464869	-1.6043866633
C	-1.2081033625	-1.7789705095	-2.7356824408
C	-1.4861090759	-3.1409676223	-0.8394650345
C	-4.3639279446	1.5560292460	-2.5630578879
C	-3.9974160103	-1.2526382799	-2.7653798146
C	-3.3090459591	1.0457759242	-3.3060622307
C	-2.2392702513	-3.3219724842	0.3125921332
C	-5.2801638986	0.6541505115	-1.8889935847
C	0.1502396590	0.7056980774	-2.5146377229
C	0.3183557754	-2.1076356883	0.4682817910
C	0.6553731823	-0.4650960375	-1.8226762227
C	-1.7999205164	2.7676578128	-2.4074613932
C	-0.0056462050	-1.6802706150	-1.9311890832
C	-5.2730094727	-1.5587809603	-0.8165658339
C	-4.2761493700	-2.6126414313	-0.8706104705
C	-3.4878477422	-2.4233875408	-2.0750043315
C	-5.1001948055	-0.7178675933	-1.9877946576
C	-3.6653930000	-3.0505139835	0.2960001940
C	-4.1567192103	2.7085532077	-1.7054177050
C	-1.0008980227	0.6111581212	-3.2837918371

References

1. M. Wijtmans, C. de Graaf, G. de Kloe, E. P. Istyastono, J. Smit, H. Lim, R. Boonnak, S. Nijmeijer, R. A. Smits, A. Jongejan, O. Zuiderveld, I. J. P. de Esch and R. Leurs, *J. Med. Chem.*, 2011, **54**, 1693-1703.
2. G. R. Fulmer, A. J. M. Miller, N. H. Sherden, H. E. Gottlieb, A. Nudelman, B. M. Stoltz, J. E. Bercaw and K. I. Goldberg, *Organometallics*, 2010, **29**, 2176-2179.
3. D. Arican and R. Brückner, *Org. Lett.*, 2013, **15**, 2582-2585.
4. A. K. Morri, Y. Thummala and V. R. Doddi, *Org. Lett.*, 2015, **17**, 4640-4643.
5. K. W. Bentley, Z. A. de los Santos, M. J. Weiss and C. Wolf, *Chirality*, 2015, **27**, 700-707.
6. H.-I. Chang, H.-T. Huang, C.-H. Huang, M.-Y. Kuo and Y.-T. Wu, *Chem. Commun.*, 2010, **46**, 7241-7243.
7. R. Berger, M. Wagner, X. Feng and K. Müllen, *Chem. Sci.*, 2015, **6**, 436-441.
8. S. Ito, Y. Tokimaru and K. Nozaki, *Chem. Commun.*, 2015, **51**, 221-224.
9. T. Nagano, K. Nakamura, Y. Tokimaru, S. Ito, D. Miyajima, T. Aida and K. Nozaki, *Chem. – Eur. J.*, 2018, **24**, 14075-14078.
10. S. Ito, Y. Tokimaru and K. Nozaki, *Angew. Chem. Int. Ed.*, 2015, **54**, 7256-7260.
11. L. K. S. von Krbek, C. A. Schalley and P. Thordarson, *Chem. Soc. Rev.*, 2017, **46**, 2622-2637.
12. P. Thordarson, *Chem. Soc. Rev.*, 2011, **40**, 5922-5923.
13. R. Neufeld and D. Stalke, *Chem. Sci.*, 2015, **6**, 3354-3364.
14. D. A. Stauffer, R. E. Barrans and D. A. Dougherty, *J. Org. Chem.*, 1990, **55**, 2762-2767.
15. CrystalClear–SM Expert (version 2.1 b45), Rigaku Americas Corp.: The Woodlands, TX, USA, 2015.
16. ABSCOR, T. Higashi, Rigaku Corp.: Tokyo, Japan, 1995.
17. O. V. Dolomanov, L. J. Bourhis, R. J. Gildea, J. A. K. Howard and H. Puschmann, *J. Appl. Crystallogr.*, 2009, **42**, 339-341.
18. G. M. Sheldrick, *Acta Crystallogr. A*, 2015, **71**, 3-8.
19. G. M. Sheldrick, *Acta Crystallogr. C*, 2015, **71**, 3-8.
20. A. L. Spek, *Acta Crystallogr. D*, 2009, **65**, 148-155.
21. C. J. Chancellor, F. L. Bowles, J. U. Franco, D. M. Pham, M. Rivera, E. A. Sarina, K. B. Ghiassi, A. L. Balch and M. M. Olmstead, *J. Phys. Chem. A*, 2018, **122**, 9626-9636.
22. M. M. Olmstead, D. A. Costa, K. Maitra, B. C. Noll, S. L. Phillips, P. M. Van Calcar and A. L. Balch, *J. Am. Chem. Soc.*, 1999, **121**, 7090-7097.
23. H. B. Burgi, E. Blanc, D. Schwarzenbach, S. Z. Liu, Y. J. Lu, M. M. Kappes and J. A. Ibers, *Angew. Chem. Int. Ed.*, 1992, **31**, 640-643.
24. S. Z. Liu, Y. J. Lu, M. M. Kappes and J. A. Ibers, *Science*, 1991, **254**, 408-410.
25. M. J. Frisch, G. W. Trucks, H. B. Schlegel, G. E. Scuseria, M. A. Robb, J. R. Cheeseman, G. Scalmani, V. Barone, B. Mennucci, G. A. Petersson, H. Nakatsuji, M. Caricato, X. Li, H. P. Hratchian, A. F. Izmaylov, J. Bloino, G. Zheng, J. L. Sonnenberg, M. Hada, M. Ehara, K. Toyota, R. Fukuda, J. Hasegawa, M. Ishida, T. Nakajima, Y. Honda, O. Kitao, H. Nakai, T. Vreven, J. A. Montgomery, Jr., J. E. Peralta, F. Ogliaro, M. Bearpark, J. J. Heyd, E. Brothers, K. N. Kudin, V. N. Staroverov, T. Keith, R. Kobayashi, J. Normand, K. Raghavachari, A. Rendell, J.

C. Burant, S. S. Iyengar, J. Tomasi, M. Cossi, N. Rega, J. M. Millam, M. Klene, J. E. Knox, J. B. Cross, V. Bakken, C. Adamo, J. Jaramillo, R. Gomperts, R. E. Stratmann, O. Yazyev, A. J. Austin, R. Cammi, C. Pomelli, J. W. Ochterski, R. L. Martin, K. Morokuma, V. G. Zakrzewski, G. A. Voth, P. Salvador, J. J. Dannenberg, S. Dapprich, A. D. Daniels, O. Farkas, J. B. Foresman, J. V. Ortiz, J. Cioslowski, D. J. Fox, Gaussian 09, Revision D.01, Gaussian, Inc., Wallingford, CT, USA, 2013.

26. Y. Zhao and D. G. Truhlar, *Theor. Chem. Acc., 2008, 120,* 215-241.
27. P. A. Denis, *Rsc. Adv.*, 2013, **3**, *2*5296-25305.
28. P. A. Denis, *Chem. Phys. Lett., 2011, **516**,* 82-87.
29. Y. Zhao and D. G. Truhlar, *Phys. Chem. Chem. Phys.*, 2008, **10**, 2813-2818.
30. Y. Zhao and D. G. Truhlar, *J. Am. Chem. Soc.*, 2007, **129**, 8440.
31. S. Grimme, J. Antony, S. Ehrlich and H. Krieg, *J. Chem. Phys.*, 2010, **132**, 154104.
32. S. Grimme, A. Hansen, J. G. Brandenburg and C. Bannwarth, *Chem. Rev.*, 2016, **116**, 5105-5154.
33. B. Brauer, M. K. Kesharwani, S. Kozuch and J. M. L. Martin, *Phys. Chem. Chem. Phys.*, 2016, **18**, 20905-20925.
34. T. Risthaus and S. Grimme, *J. Chem. Theory. Comput.*, 2013, **9**, 1580-1591.
35. M. R. Kennedy, L. A. Burns and C. D. Sherrill, *J. Phys. Chem. A*, 2012, **116**, 11920-11926.
36. S. Grimme, *Wires Comput. Mol. Sci.*, 2011, **1**, 211-228.